THE MELTING BEHAVIOUR OF EQUIAXED GRAIN BOUNDARIES

by

RAIMO NORMAN ORAVA

A THESIS SUBMITTED IN PARTIAL FULFILMENT OF
THE REQUIREMENTS FOR THE DEGREE OF
MASTER OF APPLIED SCIENCE

in the Department
of
MINING AND METALLURGY

We accept this thesis as conforming to the standard required from candidates for the degree of MASTER OF APPLIED SCIENCE.

Members of the Department of
Mining and Metallurgy

THE UNIVERSITY OF BRITISH COLUMBIA

June, 1959.

ABSTRACT

Experiments were performed on bicrystals of high-purity (99.986% and 99.9987%) tin to investigate the dependence of the melting behaviour of grain boundaries, particularly those of the "equiaxed" type, on applied stress, orientation difference, boundary orientation, growth conditions, and purity. By a comparison with previous work on columnar boundaries it was concluded that there was no structural difference between equiaxed and columnar boundaries having the same geometry. Any difference in behaviour was attributed to the build-up of impurities at the equiaxed boundary due to the zone-refining effect on growth. Calculations on the diffusion of Pb, the major impurity in Sn, show that the impurity content does not decrease appreciably in the duration of the test, and consequently could be considered constant from specimen to specimen. Thus, the melting behaviour is a property of the atomic structure of a grain boundary, quite apart from any effect due to impurities. Tilt boundaries exhibit no dependence of melting behaviour on orientation difference above 16°, whereas twist boundaries do. A peak of minimum disorder appears at 41°. The dependence is predictable from coincidence plots.

In presenting this thesis in partial fulfilment of the requirements for an advanced degree at the University of British Columbia, I agree that the Library shall make it freely available for reference and study. I further agree that permission for extensive copying of this thesis for scholarly purposes may be granted by the Head of my Department or by his representatives. It is understood that copying or publication of this thesis for financial gain shall not be allowed without my written permission.

Department of Mining and Metallurgy

The University of British Columbia,
Vancouver 8, Canada.

Date July 2, 1959.

ACKNOWLEDGEMENT

The author is grateful for financial aid in the form of research assistantship granted by the Defence Research Board of Canada.

Special thanks are extended to Dr. E. Teghtsoonian for his supervision and patience, and to Mr. R. Richter and Mr. R. Butters for their technical advice and assistance.

TABLE OF CONTENTS

Table of Contents (Cont'd.)

LIST OF ILLUSTRATIONS

List of Illustrations (Cont'd.)

LIST OF TABLES

THE MELTING BEHAVIOUR OF EQUIAXED GRAIN BOUNDARIES

1. INTRODUCTION

1.1 Object of the Investigation

The structure and properties of grain boundaries in metals have been the source of considerable interest in recent years. Studies of measureable intrinsic properties of a grain boundary have led to conclusions concerning its structure. This structure is of fundamental importance because grain boundaries have a pronounced effect on the properties of metals. Attention has been chiefly directed towards properties such as grain boundary energy, diffusion, shear, and migration. However, only as recently as 1957 have results of carefully performed experiments on the melting behaviour of grain boundaries been reported, by Weinberg and Teghtsoonian[1]. This thesis reports further observations on grain boundary melting.

1.2 Theories of Grain Boundary Structure

A grain boundary in a pure metal separates regions of ordered lattice differing in crystallographic orientation. The two earliest conceptions of the structure of a crystal boundary were the amorphous layer theory and the transitional lattice theory.

Bengough[2] and Rosenhain[3] proposed that metal grains were cemented together by a supercooled viscous liquid termed an "amorphous cement" to account for the following facts:

(i) deformation by the slip mechanism within the grains gave way to boundary sliding above a certain critical temperature near the melting point[4]. (Recall that an amorphous substance is hard and strong well below the melting point but is capable of softening more rapidly than a crystalline material as the temperature is increased.)

(ii) the transition region between grains was considered to be too thin to allow atoms to bind together as a crystalline substance.

(iii) a small stress produced intercrystalline facture a few degrees below the melting point of a polycrystal without producing appreciable distortion to the grain[5].

The thinness of the boundary was not a valid argument because of the short range of atomic forces. With this realization, Hargreaves and Hills[6] proposed a much thinner transitional lattice grain boundary model where the atoms were no longer arranged randomly as implied by the term "amorphous". A definite atomic pattern implied that the boundary in any bicrystal is reproducible with respect to crystallographic structure if the relative orientation of the two bounding crystals and the orientation of the boundary itself always remain the same. The

orientation difference dependence of grain boundary free energy[10,15], diffusion[12,13,14], and melting behaviour[1,21], provided the most incontrovertible evidence for the transitional lattice theory.

At first, the transitional lattice could not explain the ability of one grain to slip viscously over another. Mott's theory of islands of perfect lattice enclosed by regions of misfit attempted to account for intercrystalline deformation. At a critical temperature, the combined effect of the thermal energy and the misfit energy was assumed to cause localized melting. Deformation could then proceed intergranularly with neglibible slip resistance.

From the close argreement found between the activation energy for viscous intercrystalline slip and that for volume diffusion, Kê[8] concluded that the local structure of the boundary region responsible for slip was the same as the local structure of the interior of the grain responsible for volume diffusion. He proposed a boundary which consisted of disordered groups of atoms or imperfections similar to the vacant lattice sites necessary for volume diffision. Between these groups there are regions of relatively perfect lattice.

Kê pointed out that any region of disordered lattice would behave in a viscous manner. Therefore, the concept of a viscous grain boundary was consistent with not only the amorphous cement theory but also the transitional lattice theory. This allows for the viscous behaviour of the transition boundary during deformation.

A specific model for the transitional lattice was first proposed by Burgers[9]. He showed that the fit of two sets of differently oriented lattice planes could be accomplished by an array of dislocations. This is represented diagrammatically in Figure 1 for a tilt boundary in a simple cubic crystal.

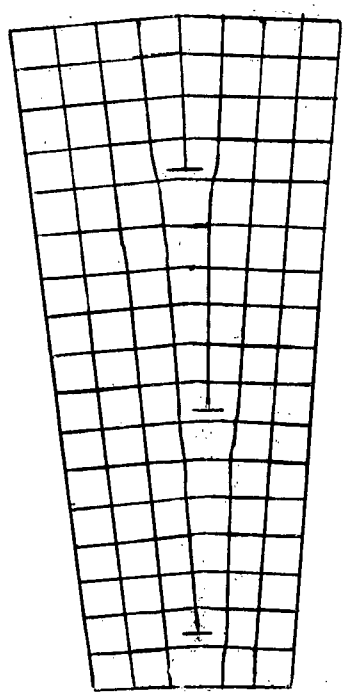

Figure 1. Simple small-angle tilt grain boundary showing the array of edge dislocations describing the boundary.

Read and Shockley[10] made an extensive study of dislocation models of grain boundaries. They obtained an expression for grain boundary energy as a function of the orientation difference, θ. Frank[11] analyzed dislocation contents as applied to a general grain boundary of arbitrary orientation difference and arbitrary orientation of the boundary. This form is restricted to small-angle boundaries because, as θ increases, the dislocations approach so close to each other that they lose their identity.

For large differences of orientation, it would appear that models such as that of Mott or Kê are more plausible descriptions of the boundary.

Another large-angle boundary model was proposed by Smoluchowski[12] as a result of the orientation dependence of grain boundary diffusion[13,14]. He suggested that a grain boundary consisted of dislocations for small angles merging into rod-like regions of misfit for intermediate orientation differences. These then coalesce into flat slabs of disorder as the condition for maximum misorientation is approached. At this maximum point, the boundary becomes a uniform layer of distorted material.

Aust and Chalmers[15] showed that the specific energy of a crystal boundary in tin was dependent on the orientation difference at the boundary, when this was less than 6°. This furnished very strong support for the transitional lattice model of the crystal.

1.3 Previous Melting Experiments

From experiments in boundary melting, Chalmers[16] concluded in 1940 that grain boundaries of tin (Chempur 99.986%) exhibited a depression in melting point of 0.14C° ± 0.005C° from the bulk melting point under the application of a tensile stress between the limits of 1000 and 3000 gm./cm.^{2}. This was true for angles of orientation difference in the range of 14° to 85°. No results were reported for θ smaller than 14° or greater than 85°. The sharp melting poing excluded the possibility of an amorphous cement boundary. The change from solid to liquid for an amorphous substance is gradual.

Chaudron, Lacombe, and Yannaquis[17] estimated a boundary melting point depression of 0.25C° in aluminum by observing boundaries melting ahead of the general interface.

Pumphrey and Lyon[18] conducted tensile tests, near the melting point, on aluminum. They found that the ultimate tensile strength dropped to a small but measureable value at a temperature of some 4 or 5 degrees below the melting point. Fracture was intercrystalline. It was concluded that boundaries melt 4° below the melting point of the crystal.

The internal friction measurements of Boulanger[19] near the melting point of aluminum and some of its alloys led him to believe that no incipient melting occurs at the grain boundaries unless caused by impurities or high stresses.

Shewmon[20] presented a thermodynamic argument showing that any difference in the melting point of a grain boundary and that of the bulk material would evolve only from nonequilibrium effects such as the nonequilibrium concentration of solute at the boundaries.

In contrast to the above work, Weinberg and Teghtsoonian[1] did not detect any depression of the melting point of the grain boundary in bicrystals of pure tin and pure aluminum. Results were reported for 99.9966% Sn, 99.999% Sn, 99.9999% Sn and 99.995% Al. For small-angle boundaries there was no tendency for the crystals to part at the boundary but preferential boundary melting did occur for large angles. The transition from non-melting to melting occurred at an orientation difference of 12° for tin, and 14° for aluminum. Boundary separation took place a finite time interval, t^*, after the specimen had reached the melting plateau. The addition of solute caused melting point depressions which agreed with those predicted from equilibrium phase diagrams. The value of t^* was dependent upon the applied stress, the heating rate, the purity of the material, and the orientation difference in the range 11°-15°.

Weinberg[21] has recently investigated the boundary melting behaviour of aluminum and zinc. The absence of a melting point depression for aluminum was confirmed within an experimental uncertainty of 0.05C° and verified in zinc within 0.020C°. In addition, boundaries in zinc did not separate for angles between 0°-26° and 108°-180°. There is an indication of a dependence of boundary melting on the boundary orientation in close-packed hexagonal metals because boundaries of angle θ behave unlike those of angle $(180-\theta)°$.

From directional melting tests on zone-refined lead and dilute alloys of tin, silver or gold in lead, Bolling and

Winegard[22] concluded that the presence of a small amount, namely 0.005-0.05%, of a second element in a pure metal enhances or even promotes grain boundary melting.

Chalmers[15] has differentiated between two types of boundary classified according to the manner in which they are produced, that is, their origin. One is familiar with columnar and equiaxed grains as they appear in a casting. Columnar boundaries delineate grains which grow side-by-side, normal to the advancing solid- liquid interface. In contrast, equiaxed boundaries are those resulting from the impingement of separately nucleated grains. Another difference between columnar and equiaxed boundaries is the mechanism by which impurities tend to segregate at the boundary. Chalmers maintained that the latter necessarily contain an excessive amount of impurities as a result of a zone-refining effect during solidification. On the other hand, there is no tendency for excessive segregation at a columnar boundary.

To date, no evidence that the intrinsic structure of a boundary depends on its origin has been published. In this thesis, the results of an investigation of the melting behaviour of equiaxed grain boundaries are reported. An attempt was made to determine whether the melting behaviour is a function of crystallographic structure, quite apart from the effect of impurity segregation at the boundary.

2. EXPERIMENTAL

2.1. Specimen Preparation

2.1.1. Material

The material used was tin obtained from the Vulcan Detinning Co. and was of two grades:

(i) Vulcan electrolytic: 99.986% Sn with Ni, Sb, Fe and Pb as the major detectable impurites.

(ii) Vulcan extra pure: 99.9987% Sn with Pb as the major detectable impurity.

Most of the tests were performed on the extra pure tin.

2.1.2. Seed Crystals

The standard seed was chosen with an orientation of (001) [110], that is, the (001) plane was initially horizontal and the [110] direction parallel to the growth direction.

All seeds were grown by a method commonly referred to as the modified Bridgman technique[16]. In detail, a single crystal, approximately 5 cm. long was placed at one end of a boat which did not react with tin. Graphite was used. A thin plate of graphite in the bottom of the boat facilitated the removal of the solidified crystal. Deviations from the standard orientation were obtained by inserting suitable pieces of graphite into the boat. Rotations about the [110] direction led to seeds which were used to produce bicrystals which contained a columnar tilt boundary. The formation of an equiaxed tilt boundary required seeds which were rotated about the [1$\bar{1}$0] direction.

The boat was allowed to heat up for a time before molten tin was poured into it. Thereupon the furnace was pulled over the boat and a short length of the seed crystal was melted. To enhance seeding the liquid adjacent to the solid-liquid interface was agitated with the end of a glass rod. After the interface had reached an equilibrium position the furnace was removed at the constant rates of either 0.3 or 1.0 mm./min. On solidification, the crystal was etched in a ferric chloride reagent (H_2O 80; HCl 10; $FeCl_3$ 10) to reveal any spurious changes of orientation, and to remove the thin oxide layer.

All cutting was done with a jeweller's saw using 2/0 blades. The cut face was etched electrolytically (H_2O 90; HCl 10) to remove any iron filings that might have come from the blade. Also, the deformed surface layer resulted, on occasion, in recrystallization when etching was omitted. Previous work has shown no detectable difference in results of tests on saw-cut and flame-cut specimens.

The heating element of the furnace consisted of nichrome strip wound around five tubular ceramic insulators attached to two transite end pieces. This core was encased in firebricks mounted on a trolley. The furnace was driven by a synchronous motor. Two speeds were obtained by utilizing two pulleys of different diameters on the output of a gear reducer.

2.1.3 Columnar Bicrystals

For ease of notation, bicrystals containing columnar boundaries are referred to as "columnar bicrystals". Similarly,

an "equiaxed bicrystal" contains an equiaxed boundary.

A columnar bicrystal was grown from two seeds, each of which differed in orientation from the standard (001) $[1\bar{1}0]$ by virtue of a rotation, in opposite sense, of $\theta/2$ about the $[1\bar{1}0]$ direction. This resulted in a symmetrical tilt boundary of orientation difference θ as illustrated in Figure 2. The growth procedure was similar to that applied to the seed crystals. The same furnace, driven at the slower speed, was used. A slow growth rate provided a boundary which was relatively straight. A high growth rate sometimes caused the boundary to curve towards the side of the specimen so that its geometry ceased to be that originally desired.

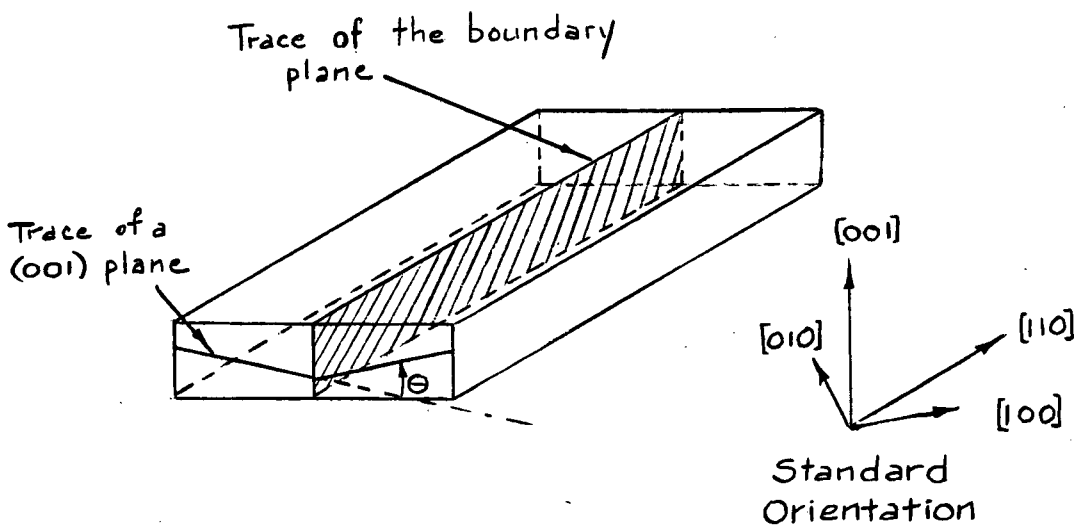

Figure 2. Columnar bicrystal containing a symmetrical tilt boundary of orientation difference $\theta°$.

The bicrystals were approximately 20 mm. wide, 5 mm. thick, and anywhere up to 100 mm. long.

2.1.4. Equiaxed Bicrystals

A problem arose here because an equiaxed boundary necessarily forms parallel to the freezing isotherm. Hence, solidification proceeds from a seed at each end of the boat towards the middle. Two basic furnace requirements had to be met:

(i) a steep temperature gradient which provides fairly sensitive control of the positions of the two solid-liquid interfaces even though the furnace remains stationary.

(ii) enough heat to melt part of the seeds.

To satisfy (i) and (ii) simultaneously is difficult because of the maximum heat that can be derived from a unit length of chromel A ribbon before it burns out. However, a satisfactory arrangement was achieved as shown in Figure 3. The heating element consists of 14 windings spaced about 2 mm. apart for a total width of 5 cm. This core is encased in two firebricks mounted on a trolley. It was necessary to make the boat supports, which serve as heat sinks, symmetrical about the middle of the boat. These consist of two pairs of brass plates, one of which can be swung out to permit the furnace to be moved away when pouring the molten metal.

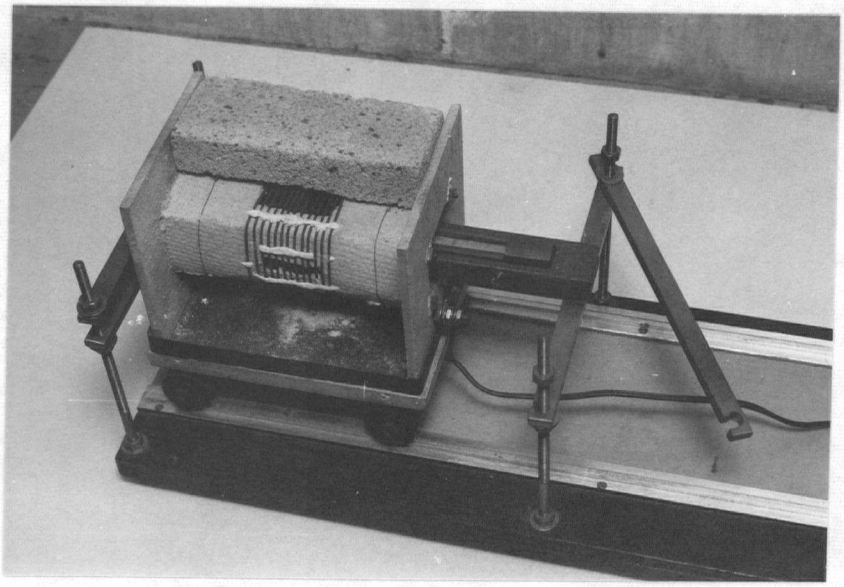

Figure 3. Furnace used for the growth of equiaxed bicrystals.

Equiaxed bicrystals were grown from two seeds, each of which differed in orientation from the standard (001) [110] by virtue of a rotation, in the opposite sense, of $\theta/2$ about the $[1\bar{1}0]$ direction. This resulted in a symmetrical tilt boundary of orientation difference θ. The [110] direction was consequently no longer oriented in the direction of growth. As a consequence, unwanted changes of orientation occurred because [110] is a preferred growth direction. A specimen containing an equiaxed boundary is illustrated in Figure 4.

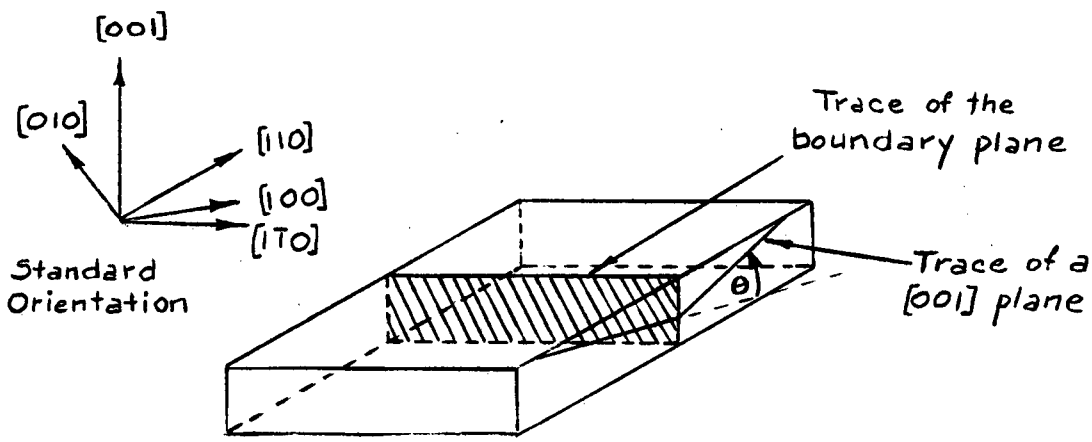

Figure 4. Equiaxed Bicrystal containing a symmetrical tilt boundary of orientation difference θ.

A graphite boat with a graphite base plate was used as previously. No particular consideration was given at first to the heat flow problem in the boat. It was assumed that the equiaxed boundary thus produced approached as closely as possible to an ideal one as formed in the equiaxed zone of an ingot. However, anomalous observations led to the investigation discussed in Section 2.4.

The bicrystals were about 18 mm. wide, 6 mm. thick and 170 mm. long.

2.1.5. Test Specimens

Test specimens 10 mm. wide were cut transversely from the columnar bicrystals to give a boundary area of 0.5 cm^2.

The equiaxed bicrystals had to be sectioned twice transversely to cut out a 20 mm. length of the bicrystal containing the boundary, and longitudinally in order to obtain two specimens 9 mm. wide. Again the boundary area was about 0.5 cm^2.

Every specimen was notched at both ends for gripping purposes. Chromel wire of gauge 32 proved strong enough. Two notches were also cut for the wire holding the specimen to the thermocouple block.

Subsequent to the cutting operations, the test specimens were etched electrolytically until the boundary became visible on the cut surface. A large scatter in experimental values on only slightly etched bicrystals made the above an essential step in the preparation.

Figure 5 shows the two types of bicrystals, and the test specimens cut from them.

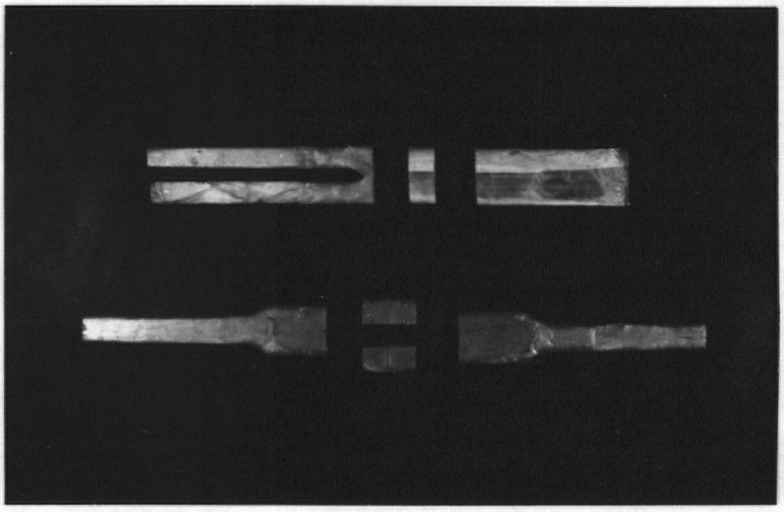

Figure 5. Top view of a columnar and an equiaxed bicrystal, showing typical test specimens.

2.1.6. Orientation Determination

The crystallographic orientation of the single and bicrystals was determined by the back-reflection Laue method[23,24]. The photographs were interpreted readily by using a Greninger chart and the standard projection of the crystal.

A colbalt target X-ray tube was used to which a voltage of 26 KV and current of 15 ma. were applied. The exposure time was 15 minutes.

The inherent uncertainty encountered in the determination of orientations by this method was found to be $\pm$ 0.5°. However, the growth of crystals from the melt will result in the disorientation of neighbouring sections by rotations of a degree or so about the growth direction. These sections may extend the entire length of a crystal but are only of the order of a mm. in dimension in the transverse direction. Consequently, the presence of such a growth imperfection, known as lineage structure, increases the error to approximately $\pm$1°. To illustrate this, five Laue photographs were taken across the 20 mm. width of one crystal of an equiaxed bicrystal, with the following results. (Table 1).

Table 1

X-ray Traverse Across an Equiaxed Bicrystal of 99.9987% Sn.

Rotation About [110]	Rotation About [1$\bar{1}$0]
1.5	23.0
1.0	23.0
2.5, 0.5	23.0, 23.0
2.0	23.0
0.5	23.5

The third exposure was particularly enlightening because it showed directly the existence of lineage. Two sets of reflections are obtained when the X-ray beam is incident on a lineage boundary.

Since the error in the determination of the crystallographic orientation of a single crystal is $\pm 1°$, the orientation difference at a columnar grain boundary may be found to within $\pm 2°$, and that of an equiaxed boundary, by its geometry, to within $\pm 0.5°$. Note that the effect of lineage on the melting behaviour of the grain boundaries is not in question at this time.

2.2. Experimental Procedure

2.2.1. Temperature Indication

A chromel-alumel thermocouple of 28 - gauge wire was cast into a tin "thermocouple block" of 99.9987% Sn, similar in size to the specimen. The junction was fused in an oxygen-gas flame and annealed at 325°C for a minimum time of one hour. This temperature was found to be critical for adequate temperature characteristics. Subsequent to annealing, 2 cm. of the end was coated with sodium silicate to insulate the bare wire from the tin. The thermocouple block had to be recast after each test, and the life of the thermocouple itself was usually three tests.

The specimen was wired to the thermocouple block. Contact between the two was established with minimum restriction to the movement of the upper crystal of the bicrystal should failure occur at the boundary.

2.2.2. Melting Apparatus

The experimental arrangement that was adopted is shown in Figure 6. Care was taken to suspend the specimen - thermocouple block symmetrically in the cavity and the same distance from the bottom each time. Failure to do this could result in an undetectable variation in the rate at which heat flows into the specimen from test to test.

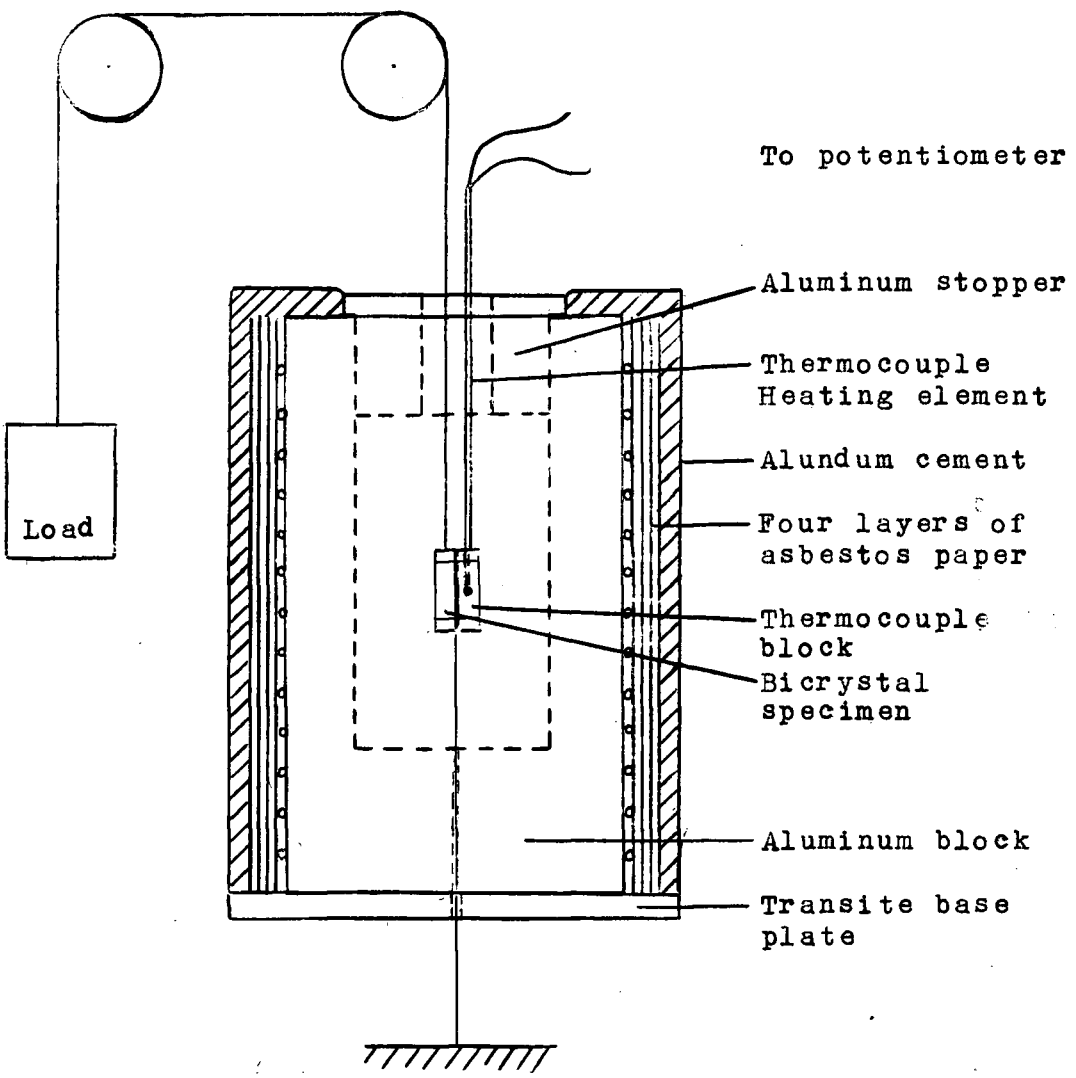

Figure 6a. Schematic representation of the melting apparatus.

Figure 6b. General view of the melting apparatus.

2.2.3. Temperature Measurement

A Pye Cambridge potentiometer and a Scalamp galvanometer were used to make the temperature measurements.

The apparatus was kept at 190°C between tests to reduce the time of heating. After the specimen was inserted, the power was increased in small increments to obtain a constant heating rate. The temperature was measured every minute up to 225°C. In the range 225°C to 231°C, the potentiometer readings were still recorded every minute. However, in addition, the galvanometer was used as a deflection instrument, with deflections being observed 30 seconds after potentiometer measurements. The latter was taken as a zero reference point for the deflections.

Above 231°C only the galvanometer scale deflections were observed at 15 second intervals until failure occurred. When

the plateau was investigated to completion the weight was not allowed to fall far enough after failure to remove the specimen from the cavity and thereby disturb its thermal state. Since this necessarily precluded visual examination the test was usually stopped immediately after separation of the bicrystal.

The galvanometer scale deflection was calibrated in μV./mm. by observing the change in deflection when the potentiometer was altered by a definite amount during a period of steady deflection.

2.2.4. Quality of the Measurements

In order that the instant at which the boundary melts be accurately determined, it was necessary to obtain a heating curve in which the rise was constant and fairly steep, the transition from rise to the plateau sharp, and the plateau flat.

The heating rate was kept constant to within 0.05 C /min. for 4 or 5 minutes before the transition point was reached. No effect of a variation from the value of 1.0 C /min. was investigated. The dependence of the time to boundary separation upon heating rate has been previously established[1].

The transition from the rise to the plateau took place within 15 seconds. The plateau was constant within 0.02 C° over a period of approximately 15 minutes at which point the thermocouple block had usually melted completely. Frequently, no deviation from the flat portion whatever was detectable on the galvanometer scale.

Another important consideration involved the verification of the initial assumption that the thermocouple imbedded in the block of tin gave the true temperature of the specimen, and,

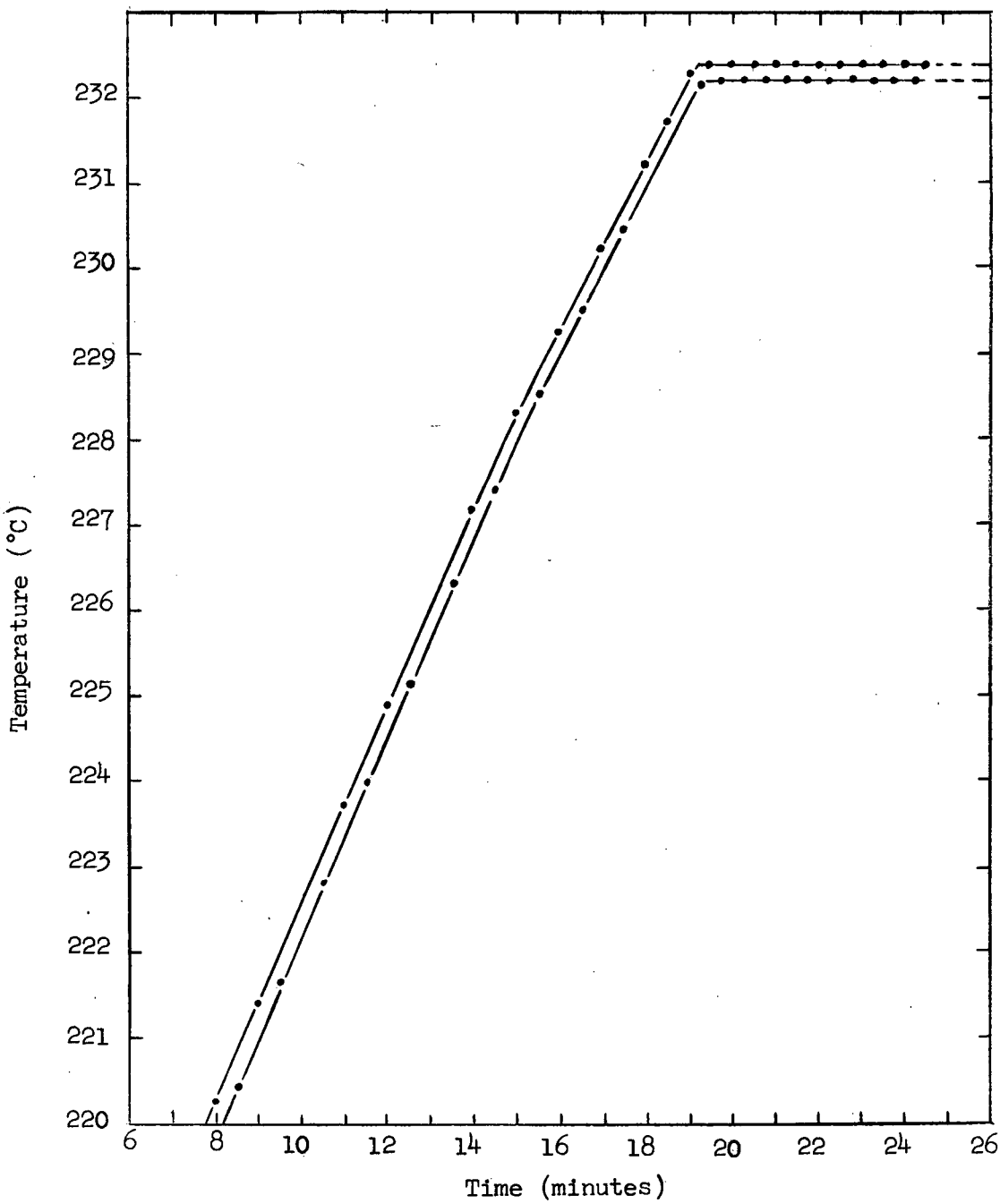

Figure 7. Heating curves for the dual thermocouple-block assembly.

thereby, of the boundary. Measurements were made on a system in which the specimen had been replaced by a second thermocouple block.

Below the melting point it was possible to read the potential of each thermocouple every minute only. On nearing the plateau switching back and forth between the two couples did not deflect the galvanometer off scale. Deflections could then be recorded at intervals of 15 seconds, and, consequently for each couple, at intervals of 30 seconds. The melting curves in Figure 7 show the parallel behaviour exhibited by the two thermocouple blocks. This indicates that either one may be used to measure the temperature of the other relative to the melting plateau. Therefore, replacement of one by a specimen was justified.

Utilizing the galvanometer as a null-indicating instrument an experimental uncertainty in potential of 1μV, and in temperature of 0.02C° was possible. By observing scale deflections the uncertainty was reduced to 0.01C°. However, this applies only to deviations from an absolute value since the deflections are based on a zero determined by null-inciation. The experimental error in the determination of the time interval, t^*, from transition to boundary separation was considered to be 0.2 minutes, or less than 15 seconds.

2.3. Observations

The failure of a specimen was indicated by the falling of the weight. Two modes of failure were observed. One was a

result of separation at the boundary and the other, excessive melting at the supports. Both occurred a finite time interval, t^*, after the onset of general melting as manifested by the plateau in the heating curve. At no time was a difference detected between the bulk melting point and the temperature at which boundary separation took place, within the stated accuracy of 0.02C°. From the appearance of those bicrystals which separated at the boundary, it was evident that little melting of the component crystals had occurred. The surface of separation at the boundary of a columnar bicrystal of 99.9987% Sn was smooth, shiny, and flat in appearance. This was independent of stress, boundary orientation, and the type of boundary, that is, tilt or twist. On occasion, a few sub-boundaries were visible, running parallel to what was originally the growth direction, [110], parallel to the boundary plane. Microscopic examination revealed the presence, in a few instances, of very localized polycrystalline regions on the surface.

A decrease in the purity of the tin from 99.9987% to 99.986% resulted in a significant change in the condition of the surface at which failure took place, namely, from smooth to irregular. The irregularity consisted of a family of ridges, running parallel to the [110] direction.

No dependence of the surface structure on the applied stress or orientation difference was found.

In the case of equiaxed boundaries, the surface of separation, even for the extra pure material, was covered with small

nipples. They became more pronounced when the impurity content was increased from 0.0013% to 0.014%, and resembled somewhat the decanted solid-liquid interface shown in Figure 11. However, the sharp boundaries which delineated the hexagonal cells of a decanted specimen were absent from the surfaces of separation of a test specimen.

The effect of stess, orientation difference, boundary orientation, purity, and growth conditions, on the melting behaviour of equiaxed boundaries is reported. One set of results on the effect of stress on the t^* values of columnar boundaries is included.

2.3.1. Stress

The stress that was applied to the test specimens ranged from 50 to 2000 gm./cm^2. It was believed that by the application of a stress in this range one could dispel the possibility of plastic deformation. The critical shear stress for β-Sn, with slip plane (110) and slip direction [001] is quoted by Barrett[25] as 13,000 gm./cm^2. Consequently, a stress of 2000 gm./cm^2. is not nearly high enough to cause slip.

For a series of tests at a constant stress level, 500 gm./cm^2. was applied.

The effect of stress on the time, t^*, to boundary separation was investigated in both equiaxed and columnar boundaries. The latter served as a tie between the results of earlier work on columnar boundaries, and this work on equiaxed boundaries.

The observations in Table 2 were made on 45° columnar tilt boundaries of 99.9987% Sn.

Table 2

Type: Columnar Tilt; Size: 45°; Purity: 99.9987%

Stress (gm./cm^2.)	t^* (min.)
50	4.0
100	3.4
200	2.6
500	1.5
"	2.0
"	1.9
"	1.0
"	1.4
"	1.4
"	1.4
1000	0.9
"	1.2
2000	0.7

The mean t^* for 500 gm./cm^2. is 1.5 min. and repeated tests fell within 30 sec. of this value. Curve I in Figure 8 illustrates the nature of the variation of t^* with applied stress. The smoothness of the curve, and the closeness of the agreement with the previously determined results plotted in Curve II was considered sufficient justification for performing only one or two tests at the other stress levels. Curve II summarizes work[1] on 45° columnar tilt boundaries of 99.999% Sn, but for a heating rate of 0.75 C°/min. instead of the 1.0 C°/min. utilized here.

Tables 3, 4 and 5 list the results of melting tests on 45° equiaxed tilt (99.9987% Sn), 41° equiaxed twist (99.9987% Sn), and 41° equiaxed twist (99.986% Sn) boundaries respectively. They are plotted in Curves III, IV and V.

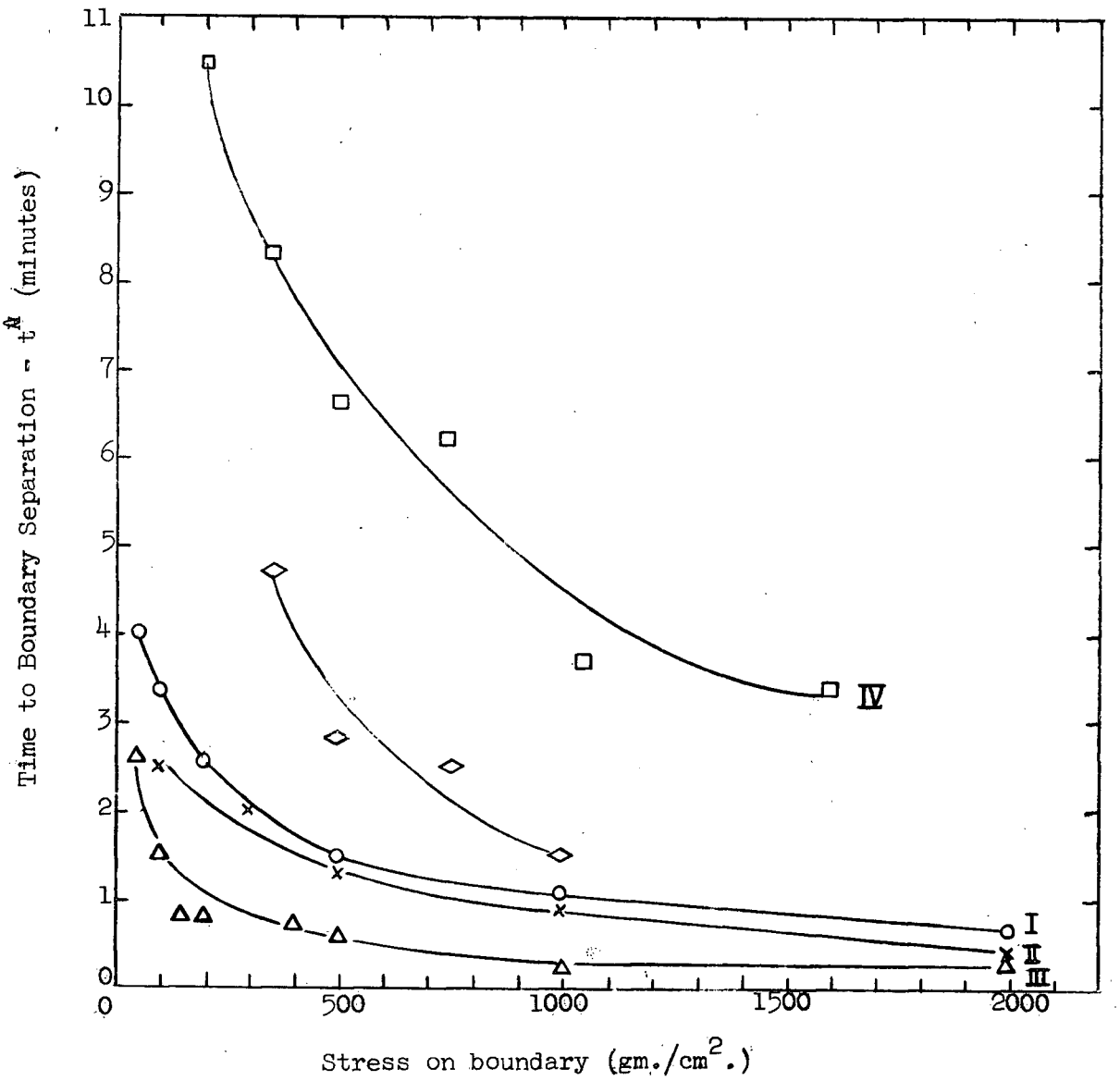

Figure 8. The stress dependence of the time to boundary separation.
I - 45° columnar tilt boundary: purity 99.9987% Sn
II - 45° columnar tilt boundary: purity 99.999% Sn (heating rate 0.75C°/min.)
III - 45° equiaxed tilt boundary: purity 99.9987% Sn
IV - 41° equiaxed twist boundary: purity 99.9987% Sn
V - 41° equiaxed twist boundary: purity 99.986% Sn

Table 3

Type: Equiaxed Tilt; Size: 45°; Purity: 99.9987% Sn

Stress (gm./cm.)	t^* (min.)
50	2.6
100	1.5
150	0.8
200	0.8
400	0.7
500	0.6
1000	0.2
2000	0.3

Table 4

Type: Equiaxed Twist; Size: 41°; Purity: 99.9987% Sn

Stress (gm./cm^2.)	t^* (min.)
200	10.5
350	8.3
500	7.0
500	6.1
750	6.2
1050	3.7
1600	3.4

Table 5

Type: Equiaxed Twist; Size: 41°; Purity: 99.986% Sn

Stress (gm./cm^2.)	t^* (min.)
350	4.7
500	2.8
750	2.2
1000	1.5

2.3.2. Orientation Difference

Tests were conducted on equiaxed tilt boundaries of 99.9987% Sn of orientation difference in a range 8° to 29°, and at approximately 45°. The results of tests on 23 specimens are tabulated in Table 6. All specimens which contained an equiaxed boundary of 12° or more separated at the boundary. Those of 11° or less failed at the grips due to general melting. On occasion, a groove was observed at the 11° boundary upon removal of the bicrystal from the melting apparatus after a grip failure.

Table 6

Type: Equiaxed Tilt; Size: Variable; Purity: 99.9987% Sn

Orientation Difference (degrees)	Stress ($gm./cm^2.$)	t^* (min.)
9.0	234	(7.3)+
9.0	187	(11.0)
8.0	183	(14.4)
8.5	163	(13.4)
8.0	1610	(0.5)
9.0	1720	(1.5)
10.0	500	(14.4)
10.0	500	(15.1)
11.0	1180	(13.2)
11.0	958	(7.4)
11.0	1130	(8.3)
11.0	2000	(no reading)
12.0	2600	no reading
12.0	1040	2.8
12.5	500	9.4
13.0	500	8.3
13.0	"	11.1
15.5	"	7.0
17.0	"	0.7
18.0	"	0.6
18.0	"	0.3
20.5	"	0.4
28.5	"	0.4

+ - Brackets indicate absence of boundary separation.

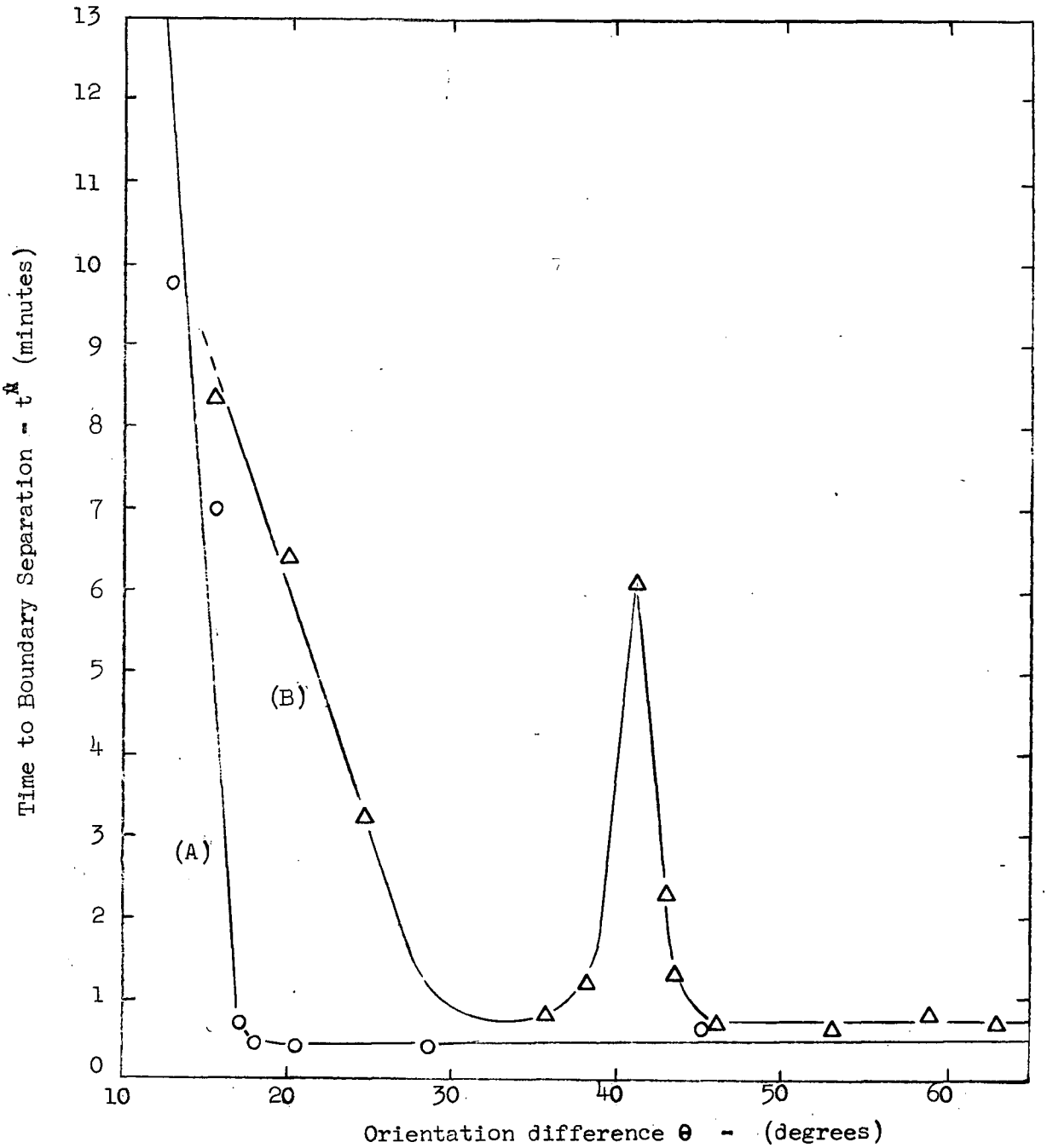

Figure 9. Orientation difference dependence of the time to boundary separation for (A) an equiaxed tilt boundary.
(B) an equiaxed twist boundary.

When the purity was reduced to 99.986% Sn, 2 out of 6 bicrystals tested in the range 9° to 10° failed by separation at the boundary (Table 7).

The length of time that a small-angled specimen remained on the melting plateau before sufficient latent heat had been supplied to cause a grip failure was approximately 15 min. This interval was independent of the applied stress, provided that the grooves for the gripping wire were cut deeply enough (over 3 wire diameters) and far enough from the end of the specimen (about 3 mm.) for effective gripping.

Table 7

Type: Equiaxed Tilt; Size: Variable; Purity: 99.986% Sn

Orientation Difference (degrees)	Stress ($gm./cm^2$.)	t^* (min.)
9.5	2230	(15.0)
9.0	1820	10.9
9.5	2090	(9.2)
9.0	1980	8.6
10.0	1090	10.7
9.5	500	15.8

Note that the preceding observations all refer to equiaxed tilt boundaries. Tests conducted on equiaxed twist boundaries of orientation difference 15° to 63°, using 99.9987% Sn yielded the results in Table 8, shown plotted in Figure 9.

Table 8

Type: Equiaxed Twist; Size: Variable; Purity: 99.9987% Sn
Constant Stress of 500 gm./cm^2.

Orientation Difference (degrees)	t* (min.)
15.5	8.4
20.0	6.4
24.5	3.2
35.5	0.8
41.0	6.1
38.0	1.2
43.0	2.3
45.5	0.7
43.5	1.3
53.0	0.6
59.0	0.8
63.0	0.7

2.3.3. Boundary Orientation

In this phase of the investigation the reference angle $\theta = 0$ corresponded to a hypothetical grain boundary where the (001) planes were parallel to the plane of the boundary. Thus the standard orientation of the seeds was chosen as $(1\bar{1}0)$ $[\bar{1}10]$ instead of (001) [110] originally specified in Section 2.1.2. This change was introduced in order to comply with Weinberg's[21] choice of a $\theta = 0$ in zinc bicrystals such that the (0001) basal planes were initially parallel to the boundary. Consequently, tests were conducted on columnar tilt boundaries of orientation difference in the range 0° to 90° based on rotations from the $(1\bar{1}0)$ $[\bar{1}10]$ standard. The range 90° to 180° has been dealt with previously[1] using tin of the same purity. The transition from boundary melting to non-melting occurred at 168°.

No boundary separation occurred at orientation differences less than 12° but did so for angles greater than 13°. The values of t^* were not measured in order to determine the possible existence of an orientation difference dependence in the range 13° to 25°. However, no detectable dependence was found between 25° and 90°.

2.3.4. Growth Conditions

Preliminary experiments showed no appreciable difference in the melting behaviour of equiaxed and columnar boundaries. At this time equiaxed bicrystals were being grown in a graphite boat containing a graphite base plate, as were columnar bicrystals. It was observed that the boundary trace on the underside of the equiaxed specimen was very irregular. As a result, the boundary no longer met the specification of symmetry. In an attempt to produce a straighter boundary the heat flow conditions in the boat were altered by the substitution of a pyrex base plate for the graphite one. Subsequently measured values of t^* did not agree with those obtained originally. Decantation experiments were performed to determine a suitable boat configuration for the formation of the most ideal equiaxed boundary possible. This is discussed in Section 2.4.

Table 9 shows the results of melting tests on equiaxed specimens grown under the various stated conditions.

Table 9

Effect of Boat Configurations on the Time to Boundary Separation

Type: Variable; Size: 45°; Purity: 99.9987% Sn

Type of Boundary	Boat Configuration	t^* (min.)
A. Columnar	Graphite boat with bottom; graphite base plate.	1.5
B. Equiaxed	As above.	1.5
C. Equiaxed	Graphite boat with bottom; pyrex base plate.	0.7
D. Equiaxed	Graphite boat with bottom removed; pyrex base plate; glass side-walls.	0.8

A variation of the rate of growth from 0.5 to 5 mm./min. had no detectable effect on the melting behaviour in 99.9987% Sn. Growth difficulties precluded the use of a higher growth rate than 5 mm./min.

2.3.5. Purity

Only one series of tests was performed to investigate the effect of purity on melting behaviour. Curves IV and V of Figure 8 show the relative effect of a small decrease in purity of the material used, from 99.9987% to 99.986%, as reported in Section 2.3.1. No depression of the melting point was detected at this lower purity.

2.4. Decantation Experiments

2.4.1. Purpose

From the observations, as cited in Section 2.3.4., it was clear that the conditions initially believed suitable for the growth of an ideal equiaxed boundary led to t^* values which agreed very well with those for columnar boundaries. To account for this similarity in behaviour, in view of the different results obtained under subsequent conditions of growth, decantations were performed at various stages of solidification for several boat configurations.

The microstructure and macroscopic form of the solid-liquid interfaces were examined in the light of the applicability of the term "equiaxed".

2.4.2. Procedure

Seeding and solification of the melt was carried out in the manner specified previously. The graphite inserts and seeds were secured by wire wound around the boat. Five boat configurations to give five different heat flow conditions were studied:

(i) graphite base plate in a graphite boat.

(ii) pyrex base plate in a graphite boat.

(iii) pyrex base plate in a bottomless graphite boat.

(iv) glass side-walls with (ii).

(v) glass side-walls with (iii).

Growth rates fell in the range of 1 to 5 mm./min.

The molten tin was poured off by tightly clamping the boat at one end, removing the furnace, and tipping the whole boat and support assembly. The time lag between the removal of the furnace and dumping did not exceed 5 seconds. Decantation was performed at a time when it was thought that the solid-liquid interfaces were as close together as possible without actually coming into contact, and, alternatively, when the interfaces were 1 to 2 cm. apart. The latter was done in order to show the shape of the advancing interfaces at an earlier stage of growth.

The two seeds had been rotated for the formation of a 28° symmetrical tilt boundary as discussed in Section 2.1.4.

The glass walls were made by cutting a microscope slide in half longitudinally. These and the pyrex base plate were coated with a fine suspension of colloidal graphite in water to prevent the solidified tin bicrystal from adhering to them.

2.4.3. Results

The effect of each of the five configurations is discussed in the order in which they were introduced.

(i) Solidification occurred preferentially adjacent to the graphite base plate. With the solid-liquid interfaces still 13 mm. apart at the top, a thickness of 1 mm. of tin joined the seeds at the bottom. The growth rate was 4 mm./min. A reduction of the rate of advancement of the interfaces to 1 mm./min. had no effect on this method of solidification. (The sketches in each sub-section illustrate the manner in which growth proceeded.)

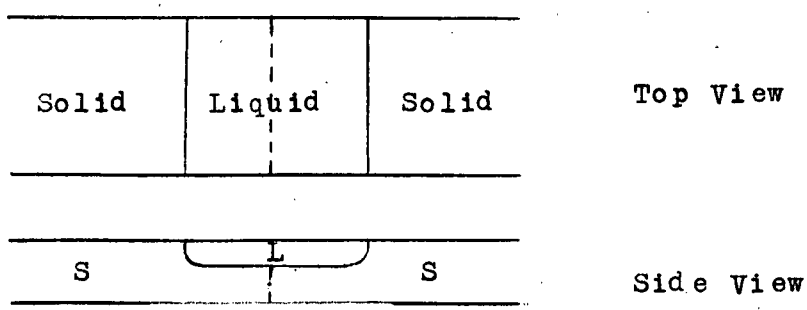

The microstructure consisted of irregularly shaped hexagonal cells over the whole decanted interface.

Upon complete solidification, the boundary trace was straight at the top surface but crooked at the bottom. It was smooth microscopically.

(ii) When the graphite base plate was replaced with a pyrex glass one, a preferential heat flow was introduced along the sides of the boat because the thermal conductivity of graphite is roughly six times that of pyrex. When the interfaces advanced at the rate of 1 mm./min. they were slightly convex into the liquid.

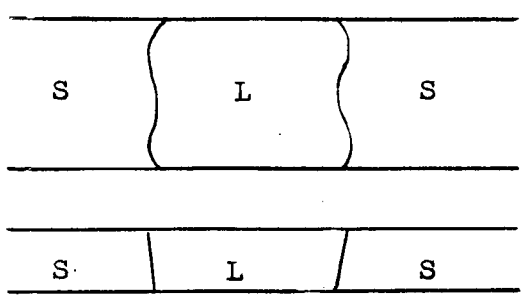

The photomicrographs in Figure 10 and 11 show the cellular substructure that is typical of the solid-liquid interfaces revealed by decanting specimens grown at rates in the specified range of 1 to 5 mm./min. Increasing the growth rate suppressed the projections at the cell centres, but did not destroy the hexagonality of the cells although it reduced them in size. The regularity of the cell geometry decreased in traversing the interface from the bottom to the top surface of the specimen.

Boundary traces were straight but saw-toothed.

(iii) The removal of the graphite bottom decreased the relative heat flow through the pyrex base plate, and resulted in the following surface contours.

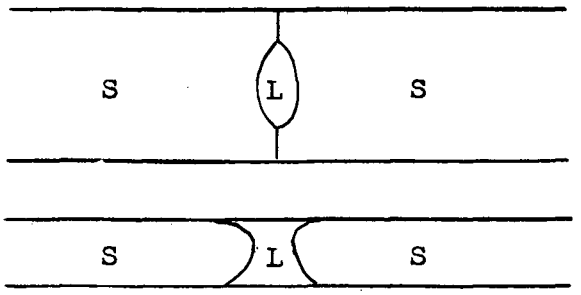

A cellular substructure was again observed at the solid-liquid interface.

(iv) The insertion of glass walls into the graphite boat with a pyrex-graphite bottom decreased the lateral heat flow through the edges but still yielded solid-liquid interfaces which had a considerable convex curvature towards the liquid.

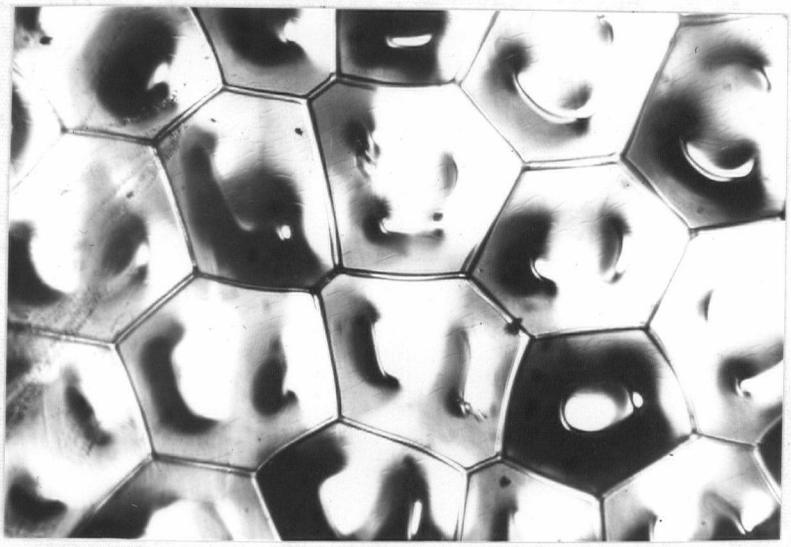

Figure 10. Decanted interface of a Sn crystal showing projections on the hexagonal cells. Growth rate: 1 mm./min.
Unetched. 100 x

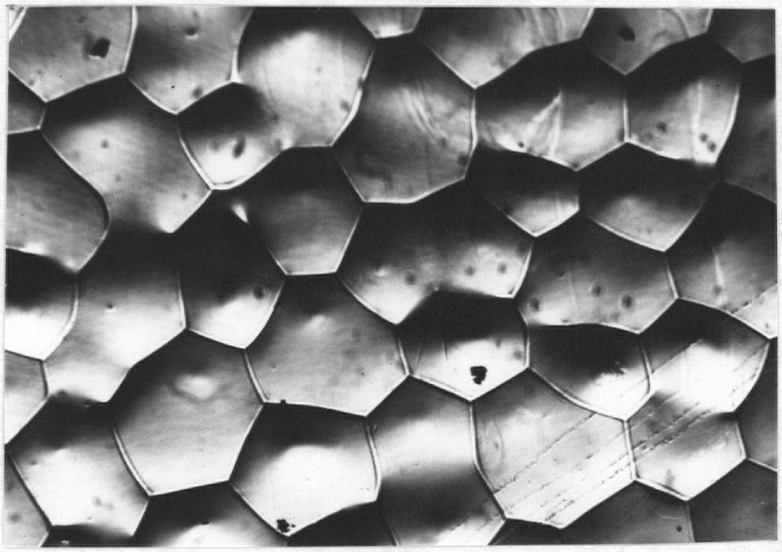

Figure 11. Decanted interface of a Sn crystal showing nipples projecting from nexagonal cells. Growth rate: 2 mm./min.
Unetched. 100 x

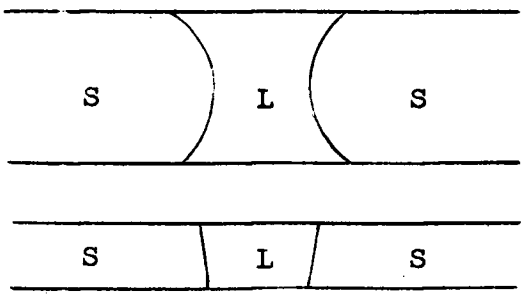

The vertical slope and microstructure remained unchanged from (ii).

(v) Recalling that the bottomless boat with a glass base plate led to preferential solidification from the edges of the specimen towards the centre, nearly planar interfaces were achieved by introducing glass sides to this system in order to reduce the relative lateral heat flow.

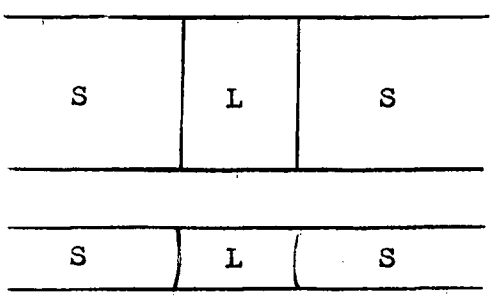

The boundary traces were still saw-toothed on the microscopic scale, but appeared straight to the eye. Hexagonal cells were observed on the decanted surface.

2.4.4. Discussion

A prismatic cellular substructure was first reported by Rutter and Chalmers[26] at the decanted interfaces of tin crystals for growth rates of 1 mm./min. and greater. There is a close agreement between the microstructure that they observed and those found in this work.

It is important that the solid-liquid interfaces which are to meet at the equiaxed boundary be as parallel as possible. Otherwise, the term "equiaxed" does not apply because solidification gives a boundary that is, in fact, grown normal to the advancing interface, technically a "columnar" boundary. Experimental results bear out the columnar nature of a boundary in a bicrystal grown under condition (i), the farthest removed from ideality. Consequently, a bottomless graphite boat, pyrex base plate and glass side-walls were utilized to grow the equiaxed bicrystals whose behaviour is to be compared with that of columnar boundaries.

3. DISCUSSION AND CONCLUSIONS

3.1. Summary of Experimental Observations

(1) The transition from the rise to the plateau of the heating curve took place within a period of 15 seconds.

(2) The melting plateau was constant to within 0.02C°, that is, a melting point depression was detectable to within 0.02C°.

(3) The error in the measurement of orientation differences was determined to be $\pm$ 1° for columnar boundaries, and $\pm$ 0.5° for equiaxed boundaries.

(4) Boundary separation occurred a finite time interval, t^*, after the onset of general melting.

(5) Boundary separation was not accompanied by appreciable melting of the component crystals.

(6) The surfaces of separation at a columnar boundary of 99.9987% Sn were smooth, shiny, and flat, with the exception of some very localized polycrystalline regions. A decrease of purity to 99.986% resulted in the presence of ridges running parallel to the growth direction.

(7) Nipples covered the separated surfaces of equiaxed boundaries, becoming more pronounced with increased impurity content.

(8) Generally, the surface structure was independent of stress, orientation difference, and type of boundary (twist or tilt).

(9) The t^* values decreased with an increase in applied stress for all boundaries.

(10) At a constant stress level, the time to boundary separation increased in the following order, according the characteristics of the boundary:

Type	Size	Purity
Equiaxed tilt	45°	99.9987% Sn.
Columnar tilt	45°	99.999% Sn. (Heating rate of 0.75 C°/min.)
Columnar tilt	45°	99.9987% Sn.
Equiaxed twist	41°	99.986% Sn.
Equiaxed twist	41°	99.9987% Sn.

Refer to Figure 8, page 26.

(11) The transition from non-separation to boundary separation occurred between 11° and 12° for both columnar and equiaxed tilt boundaries of 99.9987% Sn material.

(12) A decrease in purity to 99.986% Sn reduced the transition to somewhere between 9° and 10°.

(13) A rapid, approximately linear, decrease in t^* was observed from 12° to 17° for equiaxed tilt boundaries.

(14) A significant orientation difference dependence of t^* was evident in large-angle equiaxed twist boundaries, with a maximum t^* value occurring at 41°. The value of t^* at that point was approximately ten times that for tilt boundaries under the

same stress, and of the same orientation difference. Refer to Figure 9.

(15) The transition from non-separation to separation occurred at $\theta°$ and $(180°-\theta)°$ in columnar tilt boundaries, that is, between 11° and 12°, and 168° and 169°.

(16) A graphite boat with bottom removed, pyrex base plate and glass side-walls inserted, produced the most ideal type of equiaxed boundary.

(17) A prismatic cellular substructure was observed at the decanted interfaces of an equiaxed bicrystal.

3.2. General Discussion

It is first necessary to establish whether the occurrence of boundary separation is due to melting, or to fracture, of the boundary region. The observations of Weinberg and Teghtsoonian indicate that melting was the cause of failure at the boundary. They showed that:

(i) the visual appearance of the separated interfaces was independent of the applied stress.

(ii) boundary separation occurred at the bulk-melting point at some considerable time after the onset of general melting.

(iii) specimens of tin with added impurity exhibited a melting point depression such that separation occurred at a temperature between the solidus and liquidus temperatures according to the phase diagram of the system.

The first two observations were confirmed. In addition, localized polycrystalline areas were observed on the surfaces of some of the columnar bicrystals exposed by separation during a test. Although such regions are abundant on the exposed boundary surfaces of equiaxed bicrystals they are attributable to the existence of an internal cellular substructure, parallel to the growth direction, that is, normal to the surface. However, the presence of more than one grain at the surface of a columnar boundary seems to have no explanation other than the rapid heterogeneous solidification of a molten layer at the surface.

It now remains to determine the cause of the preferential melting at a grain boundary. Preferential melting will occur in a region whose energy relative to the rest of the lattice has been changed. The energy difference is a result of either atomic disorder due to a discontinuity in the periodicity of the lattice, or to a segregation of impurites to some region in the lattice. As it happens, a grain boundary represents just such a region, namely, having some degree of disorder, and also, at which impurity atoms tend to concentrate. For this reason, it is an interesting problem to try to differentiate between the two effects.

Note that a melting point depression was not observed, merely a preference for melting.

With this fundamental problem in mind, the effects of stress, orientation difference, boundary orientation, growth conditions, and purity are discussed in turn.

3.3. Stress

A stress was applied to the test specimens to further increase the absolute energy of the boundary. The strain energy thus introduced increases as the square of the applied stress. Sufficient strain energy is not added to lead to a measureable melting-point depression, within the experimental accuracy of 0.02 C°. It is the presence of disorder that initially promotes the preferential melting but the application of a stress enhances it a controlled amount. Consequently, the shape of the stress - t^* curves roughly follow an inverse square form. That is, the greater is the applied stress, the less time it will take to melt the boundary.

3.4. Orientation Difference

A critical orientation difference θ_c is seen to exist below which no preferential melting occurs at a boundary, and above which boundary melting is prevalent. This θ_c is the same (between 11° and 12°) for columnar and equiaxed boundaries of approximately the same purity (99.996% Sn and 99.9987% Sn respectively). Read and Shockley's[27] boundary energy equation for tin leads to a maximum at 12° corresponding favourably with θ_c. Let us assume that the columnar symmetrical tilt boundary may be represented by an array of edge dislocations which become more numerous as the orientation difference increases. Presumably then, the boundary energy, as governed by the dislocation content of a small-angle boundary, is sufficient at θ_c to induce preferential boundary melting. Once this critical energy is exceeded, the transition from non-melting to melting is sudden.

As θ increases from θ_c to 16°, a boundary energy increase is further manifested by a lowering of t^* values. At 16° the overlap of the dislocation cores, about four atomic diameters apart, is so serious that the result is a loss of identity of individual dislocations. The values of t^* remain constant from 16° to 45° so that little may be said about the nature of the tilt boundary structure above 16°.

The above discussion deals only with atomic disorder. At this stage, an equally satisfactory explanation lies in the presence of foreign atoms at the boundary, if the impurity concentration is directly related to the boundary orientation.

Curves I and III in Figure 8 indicate a difference in melting behaviour between large-angle (45°) boundaries of the columnar and equiaxed tilt orientation. The consistently lower values for the equiaxed tilt boundaries may be attributed to the presence of the impurites built up at the boundary during growth. This is discussed in Appendix I.

The equilibrium solute concentration would be the same for both types of boundary provided that their structures were identical. The method of growth of an equiaxed bicrystal necessarily forces an excess amount of impurites to the boundary region due to a zone-refining effect. Such a non-equilibrium concentration does not exist at a columnar boundary because it is grown along with the bounding crystals. However, there is little reason to believe that this concentration of impurites at an equiaxed boundary in tin decreases appreciably in the course of the time allowed for solid state diffusion. Each of

the test specimens remains at a temperature range of 220°C to 232°C for a maximum of one hour. Approximate calculations in Appendix II show that the amount of Pb, the principal impurity, diffusing away from the boundary is negligible, even after 100 hours annealing just below the melting point.

The significance of the above is that, for a given initial purity of tin, the impurity content of the boundary is constant from specimen to specimen, as closely as can be controlled by the growth conditions. Consequently, the only variable is orientation difference, that is, atomic structure. There is some question as to whether atomic structure is in fact reproducible with orientation difference once a dislocation array no longer describes the boundary. However, since the t^* values remain constant for θ constant, the structure of a large-angle tilt or twist boundary may be considered to be reproducible, whatever its structure may be. It is concluded that variations of melting behaviour with variations of orientation difference are attributable to variations of boundary geometry.

The difference in t^* values is not great from columnar to equiaxed boundaries. It is then not surprising that the transition from non-melting to melting was the same for both. The value of t^* is more sensitive to changes in purity and stress than the actual transition. For example, a variation of stress from 50 to 2000 gm/cm. does not change the transition, but alters the t^* considerably. The only evidence of the presence of an excess amount of impurites at an equiaxed boundary as far as the transition was concerned was the groove at an 11° boundary trace after grip failure.

The most interesting, and unexpected, result of the investigation was the orientation difference dependence of the melting behaviour of an equiaxed twist boundary. It was by accident that a 41° boundary was tested in the study of large-angle behaviour. Previous investigators concluded that large-angle columnar twist boundaries behave like tilt boundaries. Their tests included only 45° boundaries, whereas the peak of the curve in Figure 9 is sharp at 41° and therefore easy to miss. It is believed that this dependence is an inherent structural property of the twist boundary in tin and not of its equiaxed nature. The variation of t^* with θ is predictable from a study of the crystallography of the system made in Appendix III.

The degree of mismatch, as determined from the coincidence plots in Appendix III (Figure 13 to 16) is shown to vary with orientation difference in a similar manner to that observed experimentally. In fact, a minimum mismatch is found, theoretically, at 41°, at the exact orientation difference where the experimental peak occurred in Figure 9. A decrease in the disorder results in a decrease in boundary energy, and consequently, in a longer time interval, t^*, to boundary melting. The t^* value at 41° is approximately ten times that at 46°, and the measured mismatch at 41° is one-fifth that at 46°. The agreement is considered sufficiently close to justify the method of analysis without implying that this method of evaluating the disorder is unique.

3.5. Boundary Orientation

Since a dependence of melting behaviour on boundary orientation was found in zinc, a close-packed hexagonal metal with $c/a = 1.86$, it was thought that tin might show a similar tendency. The latter is tetragonal at room temperature up to its melting point, with $a = b$ and $c/a = 0.55$. Contrary to expectations the results indicate that the transition from non-melting to melting occurred at θ and $(180-\theta)°$, namely, about 12° and 168°. Therefore one may conclude that the atomic disorder is not detectably different at these two boundary angles, and that the melting behaviour is not a function of the boundary orientation in tin.

3.6. Growth Conditions

Refer to Section 2.4.4. for a discussion on the effect of boat configuration on melting behaviour.

From Appendix I it is evident that the growth rates utilized to grow all of the equiaxed test specimens, that is, 0.5 to 5 mm./min., led to appreciable segregation at the boundary region. Not until a rate of approximately 15 mm./min. is reached would the solute concentration at the boundary approach the mean concentration C_o, excluding any tendency for equilibrium grain boundary segregation. Difficulties in producing satisfactory bicrystals interfered with increasing the growth rate beyond 5 mm./min.

3.7. Purity

It is to be expected that the concentration of impurities at a boundary in 99.986% Sn would be more than in 99.9987% Sn.

As a consequence, the melting-point of the material in the grain boundary will be lowered, according to the phase diagram, by an amount depending on the concentration of the impurity. The concentration was at no time large enough to produce a detectable melting point depression. Nevertheless, the presence of impurities was manifested by a lowering of the t^* values and of the transition from non-melting to melting.

4. SUMMARY

The following are the main conclusions that have been reached.

(i) Equiaxed boundaries do not differ in structure from columnar boundaries. The difference in their behaviour is due to a presence of impurites built up during growth as a result of a zone-refining effect.

(ii) The variation of the melting behaviour of a grain boundary with a variation in orientation difference is primarily due to a change in the atomic structure of the boundary, with solute atoms being of secondary importance.

(iii) Large-angle twist boundaries in tin have some degree of order, unlike tilt boundaries.

(iv) Boundary melting is established as a measureable intrinsic property of a boundary, justifying its use to study boundary structure.

5. RECOMMENDATIONS FOR FUTURE INVESTIGATION

There is an absence of data on the melting behaviour of large-angle columnar twist boundaries. It is suggested that boundary melting tests be made, particularly on 41° boundaries, in order to confirm the fact that the orientation difference dependence is an inherent property of a twist boundary and not due to its equiaxed nature.

It would be revealing to investigate the whole range of θ, that is, beyond 53°. There is a suspected theoretical peak at 81°, but was not confirmed experimentally.

Since the role of impurities necessarily enters the picture, an investigation of segregation in columnar and equiaxed boundaries of varying orientation difference using radio-active tracers would be of considerable interest.

APPENDIX I

Impurity Segregation to an Equiaxed Boundary

One may calculate the effect of any growth rate on the distribution of the principal impurity Pb in Sn by using the equation[28] which describes segregation caused by normal freezing:

$$C = k\, C_o\, (1 - g)^{k - 1}$$

where C = concentration in the solid at the point where a fraction g of the original liquid has frozen.

C_o = mean conentration.

k = effective distribution coefficient.

The equilibrium distribution coefficient, k_o, is defined as the ratio of the solute concentration in the solid to the solute concentration in the liquid in equilibrium with the solid. Assume that k_o is constant and therefore calculated from the solid solubility of Pb in Sn, 2.5 weight per cent, and the eutectic composition 38.1 weight per cent. Then

$$k_o = \frac{2.5}{38.1} \approx 0.07$$

The above equation holds, theoretically, for a constant k, and constant density on freezing. Since it is impossible for k to remain unchanged over the whole range of g, the equation is only an approximation at best, particularly above $g = 0.9$.

The effective distribution coefficient k may be found from:

$$k = \frac{k_o}{k_o + (1 - k_o)\, e^{-f\delta/D}}$$

where f = growth rate, cm./sec.

δ = thickness of diffusion layer at the solid-liquid interface.

D = diffusion coefficient of the liquid.

Taking δ/D of the order 10^2, Pfann[30] shows a plot of the above equation for several values of k_o. At a growth rate of zero cm./sec., $k = k_o$. Interpolate to find any required k, given k_o and f.

Table 10

Values of the Effective Distribution Coefficient Corresponding to the Given Growth Rate, f.

f (cm./sec.)	f (mm./min.)	k
0.003	1.8	0.1
0.010	6.0	0.2
0.028	14.8	0.6

The values of C/C_o are calculated for each of these three effective distribution coefficients. The data are plotted in Figure 12 for g ranging from 0.6 to 0.99.

Table 11

Relative Impurity Concentration C/C_o Corresponding to the Given Value of the Effective Distribution Coefficient.

g	C/C_o (k = 0.1)	C/C_o (k = 0.2)	C/C_o (k = 0.6)
0.6	0.228	0.416	0.865
0.7	0.296	0.523	0.971
0.8	0.426	0.724	1.143
0.9	0.794	1.26	1.507
0.95	1.496	2.20	1.986
0.96	1.811	2.62	2.173
0.97	2.350	3.30	2.438
0.98	3.381	5.76	2.871
0.99	6.310	7.94	3.784

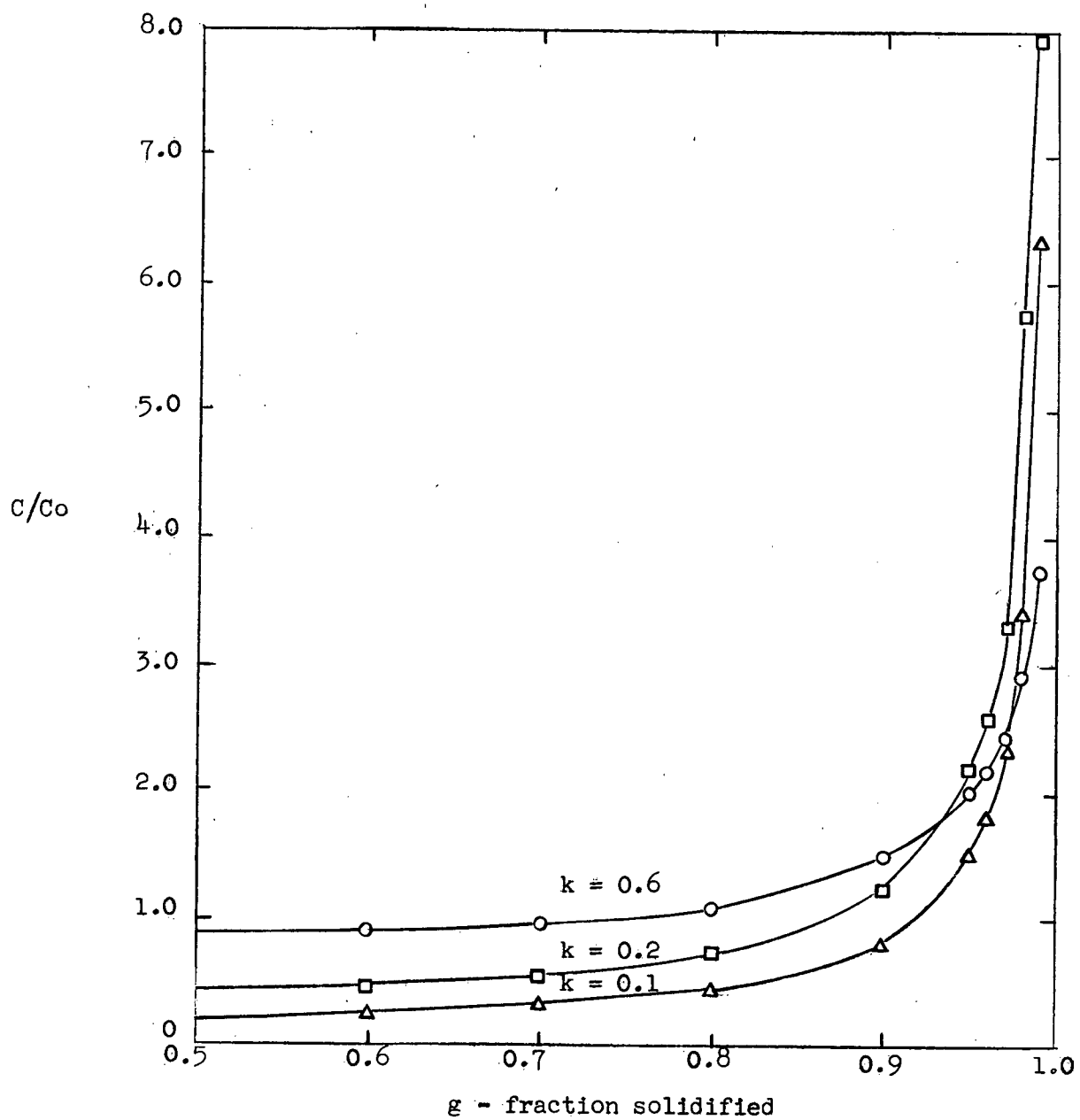

Figure 12. Curves for normal freezing.

APPENDIX II

Diffusion of Impurity from an Equiaxed Boundary

Consider the grain boundary as an infinite plane at which a total amount M of solute is deposited at time t = 0.

After a time t , and at a distance x from the boundary, the concentration is given as

$$C = \frac{M}{2\,(\pi Dt)^{1/2}} \quad e^{-x^2/Dt}$$

The concentration at the boundary after a time t is, of course, just

$$C = \frac{M}{2\,(\pi Dt)^{1/2}}$$

At time t = 0 , $\frac{C}{M}$ = 0 if x>0, and at x = 0 , $\frac{C}{M}$ is infinitely large. M is the total amount of diffusing material, and C is the concentration of impurity per amount of solvent. In the infinite boundary plane there is assumed to be no solvent at t = 0, which accounts for the value of C/M.

This solution is obtained from the diffusion equation by an analogy to the Kelvin heat-source after applying the given initial and boundary conditions.

The self-diffusion coefficient for Sn^{30} perpendicular to the c - axis ($D_\perp$) is

$3.7 \times 10^{-8}\ e^{-\ 5900/RT}\ cm^2./sec.$

and parallel to the c - axis ($D_{\parallel}$) is

$$1.2 \times 10^{-5} \, e^{-10,500/RT} \ cm^2./sec.$$

Since diffusion away from the boundary must proceed, relatively, perpendicular to the c - axis, $D_{\perp}$ is used. In addition, $D_{\perp}$ is believed to be of the correct order of magnitude for the diffusion of Pb in Sn.

A specimen remains at temperature approximately one hour before the completion of a test. Therefore, take t = 3600 seconds and x = 0. At 227°C, $D_{\perp} = 1.0 \times 10^{-10}$ cm.^{2}/sec., $\frac{C}{M} = 470$. In addition, the C/M values after 25, 50, and 100 hours are given in Table 12.

Table 12

C/M For Given Annealing Times

Time (hours)	C/M
1	470
25	94
50	60
100	47

The large values of C/M indicate that the relative concentration of the impurity Pb, at the boundary, even after 100 hours of annealing, is very high.

APPENDIX III

Coincidence Plots

The structure of tin at room temperature and above consists of two interwoven body-centered tetragonal lattices. In fact, a unit cell could be thought of as containing a body-centering atom, (1/2, 1/2, 1/2), and the following atoms in the faces: (1/2, 0, 1/4) and (0, 1/2, 3/4).

As outlined in Section 2.1.3. a rotation of the prescribed standard orientation (001) [110] about the [1$\bar{1}$0] direction produced an equiaxed tilt boundary. From the existing knowledge of tilt boundaries, as θ increases the disorder is expected to increase also without interruption until θ becomes 90°. This is borne out by the experimental results.

Now suppose one rotates each of the crystals comprising a bicrystal by small successive rotations $\theta/2$ about [110] to produce an equiaxed twist boundary. Accordingly, the (110) planes rotate but always remain parallel to the boundary. This mismatch, or disorder, is a result of this rotation. The translation of one crystal with respect to the other in a bicrystal does not alter the magnitude of the mismatch.

It is necessary first to investigate the qualitative nature of this disorder, and then assess it quantitatively. Consider the positions of the atoms in the two (110) planes adjacent to the boundary. Figure 13, for example, gives a picture of these planes considering the boundary to lie in the plane of the page. The black dots represent atoms in the (110) plane above the boundary, and the circles, atoms in the (110) plane below the

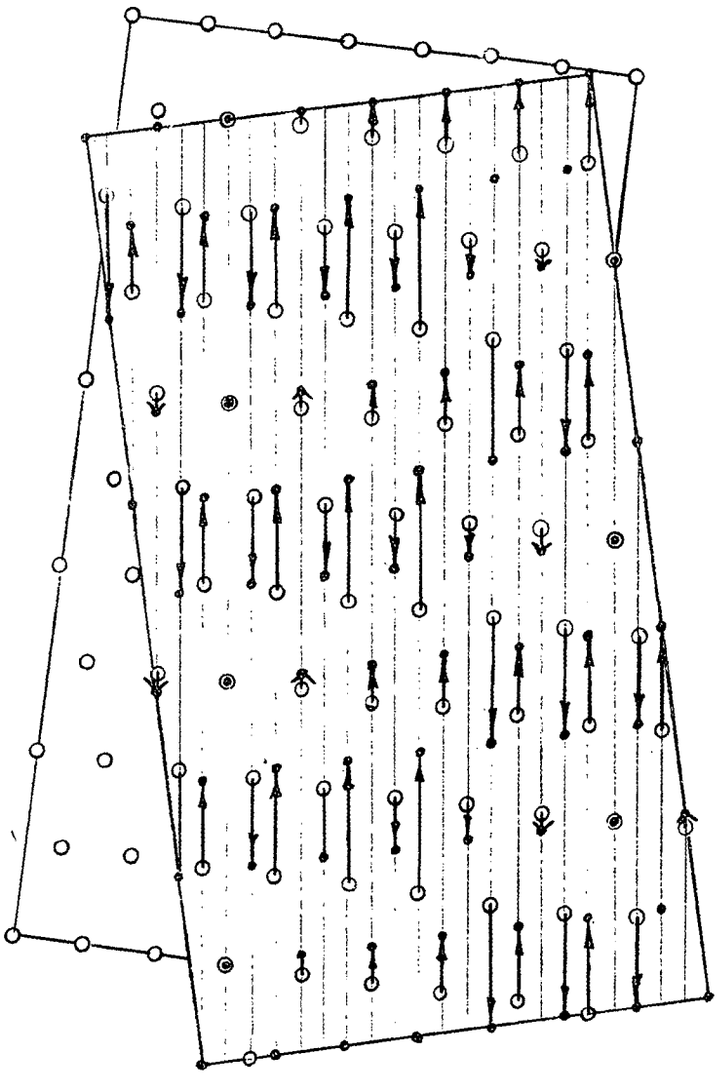

Figure 13. Coincidence plot for a 14° equiaxed twist boundary

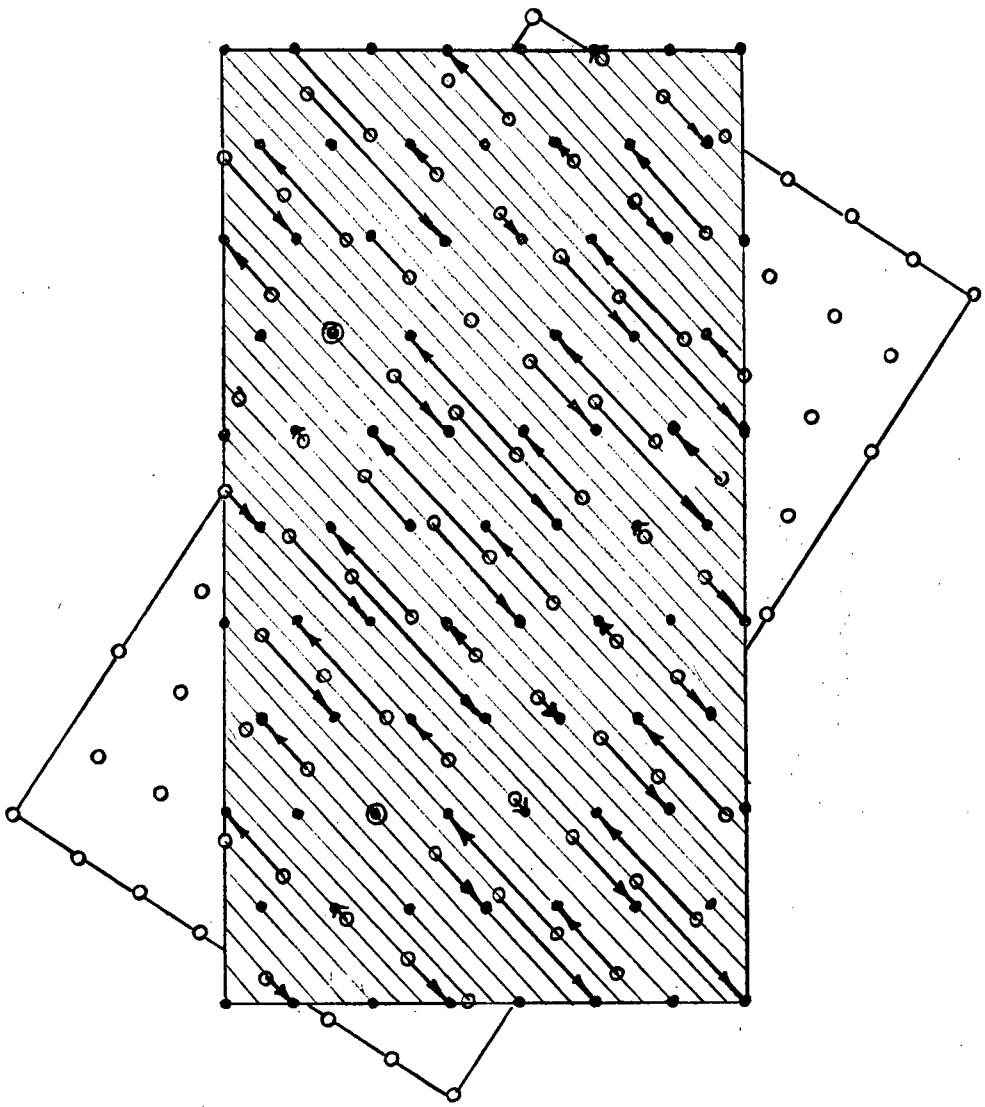

Figure 14. Coincidence plot for a 33° equiaxed twist boundary.

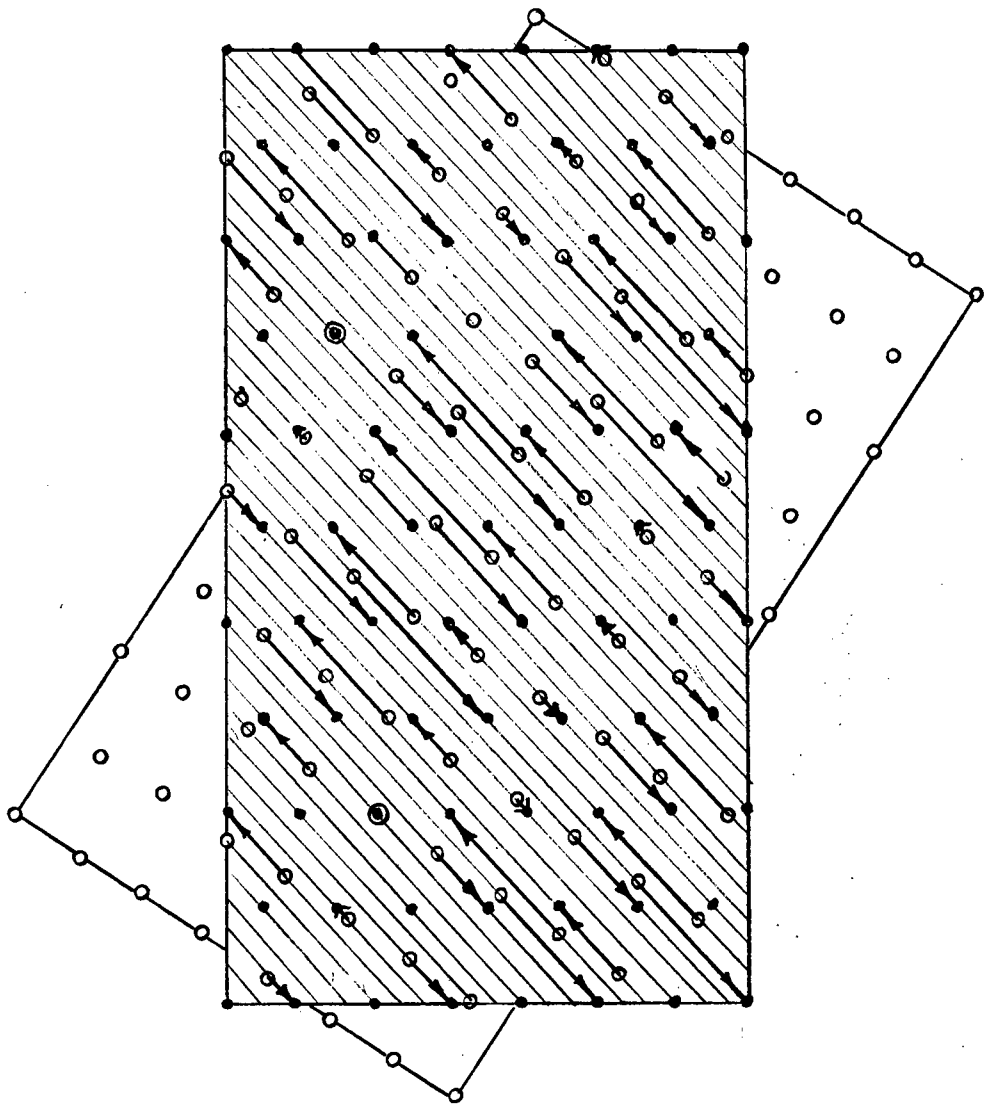

Figure 14. Coincidence plot for a 33° equiaxed twist boundary.

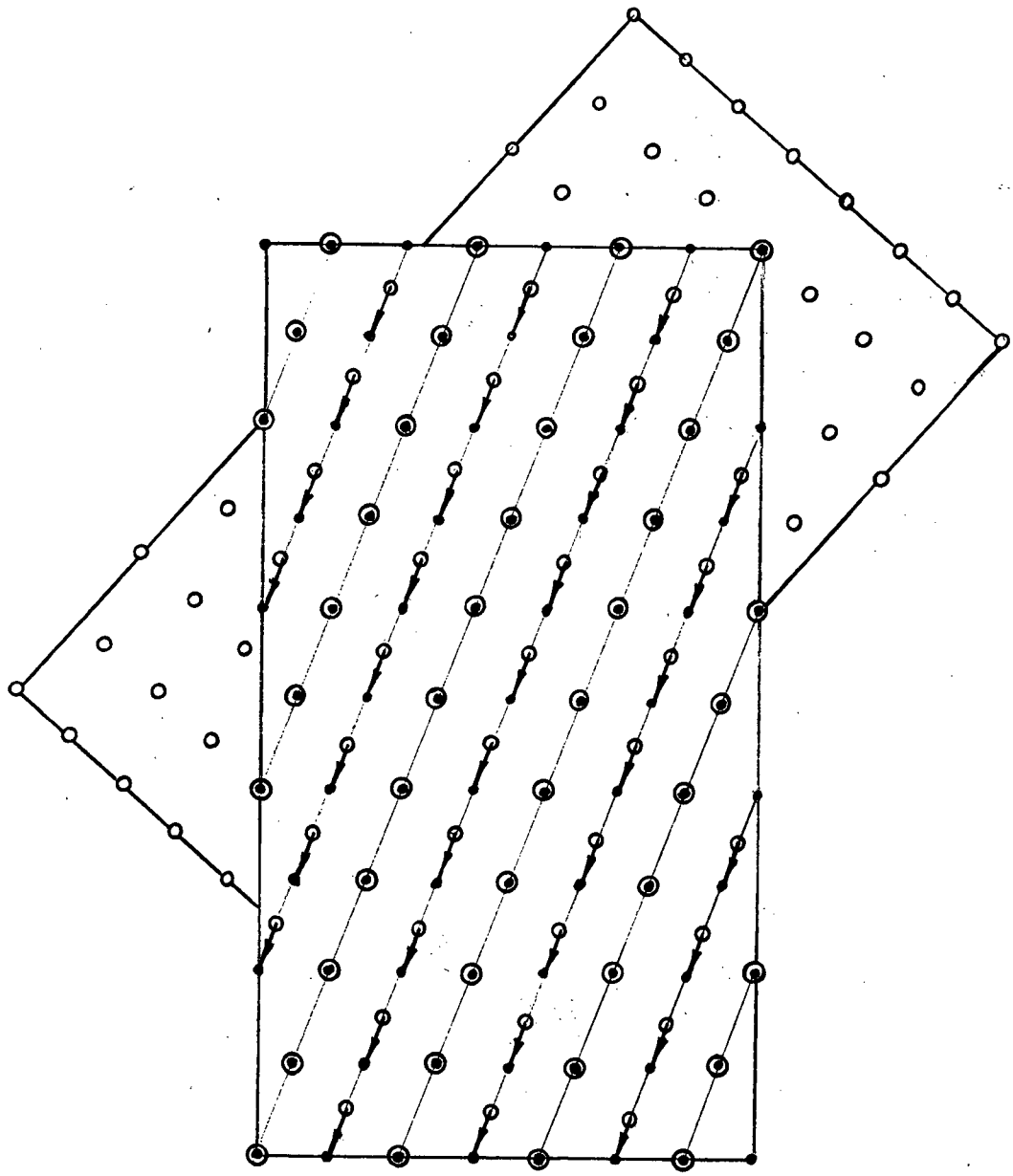

Figure 15. Coincidence plot for a 41° equiaxed twist boundary.

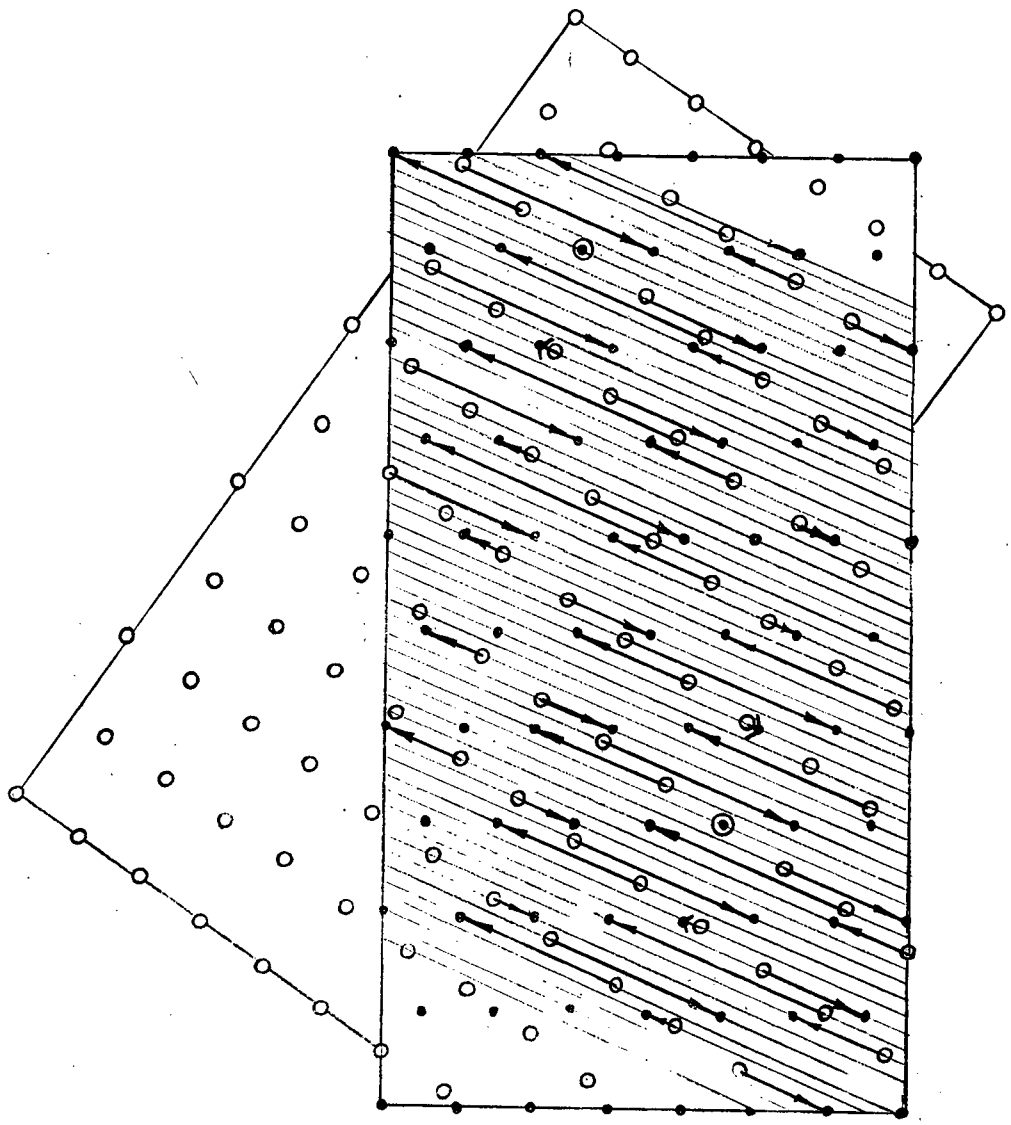

Figure 16. Coincidence plot for a 46° equiaxed twist boundary.

boundary. If one atom falls directly above the other, that is, coincidence occurs, then this is shown as a dot inside of a circle. The representations in Figures 13, 14, 15 and 16 are termed coincidence plots, for orientation differences of 14°, 33°, 41° and 46°. As θ changes, the initially perfect coincidence is destroyed to different degrees, depending on the magnitude of θ. At 41° every other atom is in coincidence, representing the minimum large-angle mismatch.

To evaluate this, the traces of a family of parallel planes perpendicular to the boundary, or page, were drawn. A family was chosen such that the distance between planes was a maximum and yet each atom in the two (110) planes fell in one of the planes. This permits one to associate one black dot with one circle, throughout the plot thereby accounting for all of the atoms in the rectangular area. Vectors are drawn between the two atoms of a pair. The vectors actually represent the projected distances between the atoms in the two planes under consideration. The lengths are summed over the rectangular plot and the average length is taken as a relative measure of the mismatch.

Table 13 gives the relative mismatch for several orientation differences.

Table 13

Relative Measure of the Disorder of a Twist Boundary

Orientation Difference (degrees)	Relative Disorder	t^* (min.)
14	1.8	9.5
33	2.5	0.7
41	0.62	6.1
46	3.1	0.7
53	2.5	0.7

BIBLIOGRAPHY

1. Weinberg, F. and Teghtsoonian, E.;
   Acta Met. 5 (1957) 455.

2. Bengough, G.D.;
   J. Inst. Metals 7 (1912) 123.

3. Rosenhain, W.;
   J. Inst. Metals 7 (1912) 178.

4. Rosenhain, W. and Humphrey, J.C.W.;
   J. Iron and Steel Inst. 87 (1913) 219.

5. Rosenhain, W. and Ewen, D.;
   J. Inst. Metals 10 (1913) 119.

6. Hargreaves, F. and Hills, R.J.;
   J. Inst. Metals 41 (1929) 257.

7. Mott, N.F.;
   Proc. Physical Society (London) 60 (1948) 391.

8. Kê, T.S.;
   J. Applied Physics 20 (1949) 274.

9. Burgers, J.M.;
   Proc. Physical Society 52 (1940) 23.

10. Read, W.T. and Shockley, W.;
    Physical Review 78 (1950) 275.

11. Frank, F.C.;
    Carnegie Institute of Technology Symposium on the Plastic Deformation of Crystalline Solids (1950) 150.

12. Smoluchowski, R.;
    Physical Review 87 (1952) 482.

13. Achter, M.R. and Smoluchowski, R.;
    J. Applied Physics 22 (1951) 1260.

14. Turnbull, D. and Hoffman, R.E.;
    Acta Met. 2 (1954) 419.

15. Aust, K.T. and Chalmers, B.;
    Proc. Royal Society (London) A201 (1950) 210.

16. Chalmers, B.;
    Proc. Royal Society (London) A175 (1940) 100.

17. Chaudron, G., Lacombe, P., and Yannaquis, N.;
    C.R. Acad. Sci., Paris 226 (1948) 1372.

18. Pumphrey, W.I. and Lyon, J.V.;
J. Inst. Metals 82 (1953) 33.

19. Boulanger, C.;
Revue Métal 51 (1954) 210.

20. Shewmon, P.;
Acta Met. 5 (1957) 335.

21. Weinberg, F.;
Acta Met. 6 (1958) 535.

22. Bolling, G.F. and Winegard, W.C.,
Acta Met. 5 (1957) 681.

23. Barrett, C.S.;
"Structure of Metals" (1952) 185,
McGraw-Hill.

24. Cullity, B.D.;
"X-Ray Diffraction" (1956) 215,
Addison Wesley.

25. Barrett, C.S.;
"Structure of Metals" (1952) 347,
McGraw-Hill.

26. Rutter, J.W. and Chalmers, B.;
Canadian J. Physics 31 (1953) 15.

27. Read, W.T. Jr., and Shockley, W.;
"Imperfections in Nearly Perfect Crystals" (1952) 352,
Wiley.

28. Pfann, W.G.;
"Zone Melting" (1958) 10,
Wiley.

29. Crank, J.;
"Mathematics of Diffusion" (1956) 9,
Oxford.

30. Smithells, C.J.;
"Metals Reference Book", Vol. 2, (1955) 558,
Butterworths Scientific Publications.